Optimal Laypunov Exponent Parameters for Stability Analysis of Batch Reactors with Model Predictive Control

Walter Kähm, Vassilios S. Vassiliadis*

Department of Chemical Engineering and Biotechnology, Process Systems Engineering Group, University of Cambridge, West Cambridge Site, Philippa Fawcett Drive, CB3 0AS Cambridge, UK

Abstract

Thermal runaways in exothermic batch reactions are a major economic, health and safety risk in industry. In literature most stability criteria for such behaviour are not reliable for nonlinear non-steady state systems. In this work, Lyapunov exponents are shown to predict the instability of highly nonlinear batch processes reliably and are hence incorporated in standard MPC schemes, leading to the intensification of such processes. The computational time is of major importance for systems controlled by MPC. The optimal tuning of the initial perturbation and the time frame reduces the computational time when embedded in MPC schemes for the control of complex batch reactions. The optimal tuning of the initial perturbation and time horizon, defining Lyapunov exponents, has not been carried out in literature so far and is here derived through sensitivity analyses. The computational time required for this control scheme is analysed for the intensification of complex reaction schemes.

Keywords: optimal Lyapunov exponent parameters, thermal stability analysis, model predictive control, batch reactors

Nomenclature

Roman Symbols

Symbol	Description
$\Delta H_{r,i}$	enthalpy of reaction i $\left[\mathrm{kJ\ mol^{-1}}\right]$
$[\mathrm{A}]$, $[\mathrm{B}]$, $[\mathrm{C}]$	concentration of component A, B and C, respectively $\left[\mathrm{kmol\,m^{-3}}\right]$
A	heat transfer area $[\mathrm{m^2}]$
C_{pj}	heat capacity of component j $\left[\mathrm{J\,kg^{-1}\,K^{-1}}\right]$
C_p	heat capacity of reaction mixture $\left[\mathrm{J\,kg^{-1}\,K^{-1}}\right]$

*Corresponding Author
Email address: vsv20@cam.ac.uk (Vassilios S. Vassiliadis)

$E_{a,i}$	activation energy of reaction i $\left[\mathrm{J\ mol^{-1}}\right]$
$k_{0,i}$	pre-exponential Arrhenius constant for reaction i $\left[\left(\mathrm{m^3\,kmol^{-1}}\right)^{n-1}\ \mathrm{s^{-1}}\right]$
K_p	proportional parameter for PI control $\left[\mathrm{m^3\,s^{-1}\,K^{-1}}\right]$
$n_{\mathrm{A},i}$, $n_{\mathrm{B},i}$	reaction orders of components A and B for reaction i, respectively [−]
q_C	volumetric folw rate of coolant $[\mathrm{m^3\,s^{-1}}]$
R	universal molar gas constant $\left[\mathrm{J\ mol^{-1}\,K^{-1}}\right]$
r_i	rate of reaction i $\left[\mathrm{kmol\,m^{-3}s^{-1}}\right]$
t	time of simulation [s]
t_{lyap}	Lyapunov time horizon [s]
T_R, T_C, T_{sp}	temperature of reactor contents, coolant and reaction set-point, respectively [K]
U	heat transfer coefficient $\left[W\,\mathrm{m^{-2}\,K^{-1}}\right]$
V_R, V_C	volume of the reactor and the cooling jacket, respectively $[\mathrm{m^3}]$
y_j, $\bar{y}_j$, $\hat{y}_j$	mass fraction, mole fraction and volume fraction of component j, respectively [−]

Greek Symbols

Symbol	**Description**
ϵ	initial perturbation for Lyapunov exponents [−]
η, κ	orders of reaction for nitration of toluene [−]
Λ, Λ_{l}	Lyapunov exponent and local Lyapunov exponent $[\mathrm{s^{-1}}]$
λ_j	thermal conductivity of component j $\left[\mathrm{W\,m^{-1}\,K^{-1}}\right]$
μ_j	viscosity of component j [Pa s]
Φ	objective function for MPC algorithm [−]
ρ, ρ_C	density of reactor contents and coolant, respectively $\left[\mathrm{kg\ m^{-3}}\right]$
τ_I	integral parameter for PI control $[\mathrm{K\,s^2\,m^{-3}}]$

1. Introduction

Thermal runaways are a phenomenon which is still observed today, causing significant safety hazards and large economic loss (Theis, 2014). In industry a thermal runaway reaction can result in the stoppage of normal operation, as well as release of chemicals in order to reduce the reactor pressure. Reducing the risk of such interruptions of normal operation is therefore of major interest to industry. Increasing the temperature of the reaction system whilst keeping it under control can potentially give large improvements in process efficiency and safety. Therefore a thorough analysis of the behaviour of such exothermic systems is necessary.

The implementation of Model Predictive Control (MPC) with an embedded stability criterion was achieved in Kähm and Vassiliadis (2018b), Kähm and Vassiliadis (2018a) and Rossi et al. (2015). These implementations enabled an increased efficiency of exothermic batch processes while keeping the process under control at all times.

In Rossi et al. (2015) a boolean variable which gives rise to the system stability is determined by an algorithm. As is the case for barrier functions (Nocedal and Wright, 2006) the boolean variable causes a severe increase in the objective function if the system is deemed to be unstable. The evaluation of the boolean is system specific and therefore needs extensive trial and error. Furthermore, a badly scaled problem can occur, as the additional term in the objective gives a sharp increase close to instability.

A good review on stability criteria embedded in MPC algorithms for continuous systems is given in Albalawi et al. (2018). The work presented therein is useful for many continuous systems in industry. As in this work batch reactors are considered these criteria cannot be transferred easily to the case studies considered in this work.

In Kähm and Vassiliadis (2018b) a new stability criterion for exothermic batch reactors was introduced, which does not suffer from this issue. Furthermore, the methodology presented in this work with Lyapunov exponents is similar to that shown in Kähm and Vassiliadis (2018b), but derived using different numerical techniques.

Lyapunov exponents quantify the chaotic nature of processes by measuring the divergent or convergent nature with respect to the relevant system variables (Strozzi and Zaldívar, 1994; Melcher, 2003). This work focuses on the extension of Lyapunov exponents, based on the work given in Kähm and Vassiliadis (2018a).

Other stability criteria are present in literature, as was discussed in Kähm and Vassiliadis (2018b) and Kähm and Vassiliadis (2018a). It was shown in both that the commonly used divergence criterion does not give reliable predictions on system stability for nonlinear non-steady-state processes. Therefore these criteria are not discussed further in this work.

In literature most nonlinear MPC schemes implement a linearisation of the system present,

with which a linear MPC scheme can be used (Rawlings and Mayne, 2015). With such a formulation the stability of the closed-loop system can be proven theoretically by the use of Lyapunov functions (DeHaan and Guay, 2010; Huang et al., 2012). If no Lyapunov function can be found, end-point constraints are often employed for a very large prediction horizon. For complex and highly nonlinear systems this leads to higher computational cost as the system has to be simulated for a larger time frame. The use of an online stability criterion can reduce the time frame used by giving an indication of the system's stability at each point of the simulation.

This work aims to achieve the following goals:

- derive the optimal value for the initial perturbation ϵ for the numerical calculation of Lyapunov exponents
- determine the time horizon t_{lyap} for reliable stability prediction using Lyapunov exponents
- explore the computational time of Lyapunov exponents embedded in MPC schemes for the intensification of batch processes

Achieving these goals leads to MPC schemes which can keep nonlinear non-steady-state systems under control while intensifying the process, reaching target conversion in shorter processing time and making batch processes more efficient.

This paper is organised as follows: in Section 2 the underlying system equations and reaction schemes used for the detailed analysis of Lyapunov exponents are introduced. This is followed by Section 3, where an in-depth sensitivity analysis of the initial perturbation ϵ and time horizon t_{lyap} defining Lyapunov exponents, as well as their optimal values are presented. In Section 4 the computational time of implementing Lyapunov exponents within MPC schemes is compared to current nonlinear MPC schemes and the possibility of intensifying batch processes is presented. The key findings and prospects for future work are summarised in Section 5.

2. Process model

2.1. Reaction kinetics

The reactions analysed in this work occur in a homogeneous liquid solution and are assumed to be irreversible.

2.1.1. Reaction scheme 1: single reaction

Reaction scheme 1 corresponds to a single reaction given by the following equation:

$$\nu_{\mathrm{A},1}\,\mathrm{A} + \nu_{\mathrm{B},1}\,\mathrm{B} \rightarrow \nu_{\mathrm{C},1}\,\mathrm{C} \tag{2.1}$$

The reaction kinetics for this reaction scheme is dependent only on the concentration of components A and B and their respective orders of reaction $n_{\mathrm{A},1}$ and $n_{\mathrm{B},1}$. The rate of reaction is given by:

$$r_1 = k_{0,1} \exp\left(\frac{-E_{a,1}}{R T_R}\right) [\mathrm{A}]^{n_{\mathrm{A},1}}\ [\mathrm{B}]^{n_{\mathrm{B},1}} \tag{2.2}$$

where [A] and [B] are the concentrations of components A and B, $E_{a,1}$ is the activation energy of reaction 1, T_{R} is the reactor temperature, R is the universal molar gas constant and $k_{0,1}$ is the pre-exponential Arrhenius constant for reaction 1.

2.1.2. Reaction scheme 2: series reactions

Reaction scheme 2 consists of the reaction shown in Reaction scheme 1, as well as a second reaction in running in series. This is given by:

$$\nu_{\mathrm{A},1}\,\mathrm{A} + \nu_{\mathrm{B},1}\,\mathrm{B} \rightarrow \nu_{\mathrm{C},1}\,\mathrm{C} \tag{2.3}$$

$$\nu_{\mathrm{A},2}\,\mathrm{A} + \nu_{\mathrm{C},2}\,\mathrm{C} \rightarrow \nu_{\mathrm{D},2}\,\mathrm{D} \tag{2.4}$$

The rate of the first reaction is given by Equation (2.2). The rate of the second reaction can be described with an Arrhenius expression (Davis and Davis, 2003), including the order of reaction $n_{\mathrm{A},2}$ and $n_{\mathrm{C},2}$ with respect to reactants A and C, respectively. This expression is given by:

$$r_2 = k_{0,2} \exp\left(-\frac{E_{a,2}}{R T_R}\right) \times [\mathrm{A}]^{n_{\mathrm{A},2}}\,[\mathrm{C}]^{n_{\mathrm{C},2}} \tag{2.5}$$

The parameters have the same meaning as for reaction scheme 1, but the numerical values differ.

2.1.3. Industrial reaction: Nitration of toluene

The reaction of the nitration of toluene is an example of a complex industrial reaction carried out in batch reactors (Halder et al., 2008). The reaction is initiated by the formation of a nitronium ion $\left(\mathrm{NO_2^+}\right)$, proceeded by 3 parallel reactions with toluene:

$$\mathrm{HNO_3 + H_2SO_4} \rightarrow \quad \mathrm{NO_2^+ + HSO_4^- + H_2O} \quad (1) \tag{2.6a}$$

$$\mathrm{NO_2^+ + C_7H_8} \rightarrow \quad \text{o-}\mathrm{C_7H_7NO_2 + H^+} \quad (2) \tag{2.6b}$$

$$\mathrm{NO_2^+ + C_7H_8} \rightarrow \quad \text{p-}\mathrm{C_7H_7NO_2 + H^+} \quad (3) \tag{2.6c}$$

$$\mathrm{NO_2^+ + C_7H_8} \rightarrow \quad \text{m-}\mathrm{C_7H_7NO_2 + H^+} \quad (4) \tag{2.6d}$$

where the letters o-, p- and m- stand for ortho, para and meta positions of the nitronium ion on toluene (Mawardi, 1982). For simplification, the reactions in Equations (2.6) are hereafter reffered to as reactions $(1)-(4)$. Each of reactions $(2)-(4)$ depends on the concentration of the nitronium ion and toluene. Furthermore, as the energetics of each reaction is similar, it is assumed that the activation energy and enthalpy of reaction are equal for reactions $(2)-(4)$. The kinetic rates, on the other hand, are different: as described in Mawardi (1982) the product of such a reaction will form a molar mixture of 60% ortho-, 37% para-, and 3% meta-nitrotoluene.

Each individual reaction can be described by Arrhenius rate expressions. The reaction rates are given by the following expressions:

$$r_1 = k_{0,1} \exp\left(\frac{-E_{a,1}}{RT_R}\right) \times [\mathrm{HNO_3}]^{\eta_1} \times [\mathrm{H_2SO_4}]^{\kappa_1} \tag{2.7}$$

$$r_2 = k_{0,2} \exp\left(\frac{-E_{a,2}}{RT_R}\right) \times \left[\mathrm{NO_2^+}\right]^{\eta_2} \times [\mathrm{C_7H_8}]^{\kappa_2} \tag{2.8}$$

$$r_3 = k_{0,3} \exp\left(\frac{-E_{a,3}}{RT_R}\right) \times \left[\mathrm{NO_2^+}\right]^{\eta_3} \times [\mathrm{C_7H_8}]^{\kappa_3} \tag{2.9}$$

$$r_4 = k_{0,4} \exp\left(\frac{-E_{a,4}}{RT_R}\right) \times \left[\mathrm{NO_2^+}\right]^{\eta_4} \times [\mathrm{C_7H_8}]^{\kappa_4} \tag{2.10}$$

where η and κ are orders of reaction with respect to each reagent.

2.2. Mass and energy balances for batch reactors

A diagram of the batch reactor considered in the following simulations is shown in Figure 1.

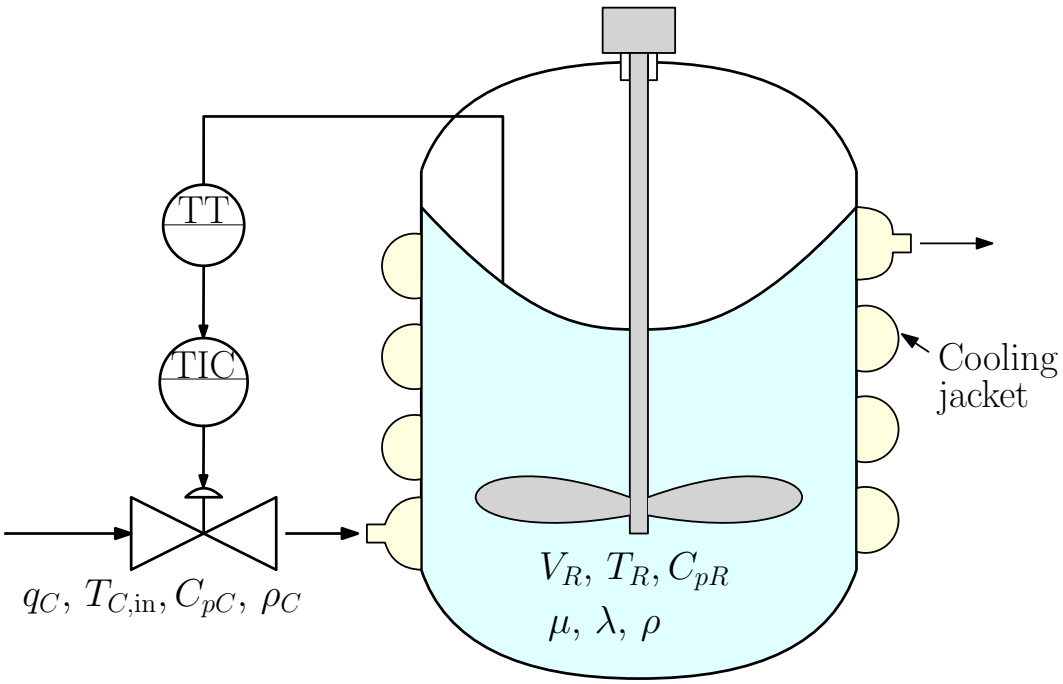

Figure 1: Batch reactor diagram for simulated systems.

For all following equations reaction scheme 2 is considered as an example. The mass and energy balances for all remaining reaction schemes are adjusted accordingly.

The overall mass balance with respect to time t is given by:

$$\frac{\mathrm{d}\left(\rho V_R\right)}{\mathrm{d}t} = 0 \tag{2.11}$$

where ρ is the reaction mixture density and V_R is the reactor volume.

The mass balance for each reagent and product is given by:

$$\frac{\mathrm{d}\left[\mathrm{A}\right]}{\mathrm{d}t} = -\nu_{\mathrm{A},1} r_1 - \nu_{\mathrm{A},2} r_2 \tag{2.12}$$

$$\frac{\mathrm{d}\left[\mathrm{B}\right]}{\mathrm{d}t} = -\nu_{\mathrm{B},1} r_1 \tag{2.13}$$

$$\frac{\mathrm{d}\left[\mathrm{C}\right]}{\mathrm{d}t} = \nu_{\mathrm{C},1} r_1 - \nu_{\mathrm{C},2} r_2 \tag{2.14}$$

$$\frac{\mathrm{d}\left[\mathrm{D}\right]}{\mathrm{d}t} = \nu_{\mathrm{D},2} r_2 \tag{2.15}$$

where r_1 and r_2 are the reaction rates given by Equations (2.2) and (2.5).

The energy balance of the reaction mixture is given by:

$$\frac{\mathrm{d}}{\mathrm{d}t}\left(\rho V_R C_p T_R\right) = r_1\left(-\Delta H_{r,1}\right) V_R + r_2\left(-\Delta H_{r,2}\right) V_R - U A \left(T_R - T_C\right) \tag{2.16}$$

where C_p is the reaction mixture heat capacity, $\Delta H_{r,1}$ and $\Delta H_{r,2}$ are the reaction enthalpy for each reaction, U is the heat transfer coefficient from reactor contents to the cooling jacket, A is the heat transfer area of the cooling jacket, and T_C is the coolant temperature.

The energy balance for the cooling jacket is given by:

$$\frac{\mathrm{d}}{\mathrm{d}t}\left(V_C\, \rho_C\, C_{pC}\, T_C\right) = q_C\, \rho_C\, C_{pC}\left(T_{C,in} - T_C\right) + U\, A\, \left(T_R - T_C\right) \tag{2.17}$$

where V_C is the cooling jacket volume, ρ_C is the coolant density, C_{pC} is the coolant heat capacity and $T_{C,in}$ is the coolant inlet temperature.

2.3. Process parameters

The parameters specific to the reaction kinetics and energy produced are varied to get a range of processes, for which the stability is analysed. The different processes are denoted by P_c^d for process c of reaction scheme d. Below the various process parameters are shown.

2.3.1. Reaction scheme 1

The process parameters for reaction scheme 1 are summarised in Table 1.

Table 1: Process parameters for reaction scheme 1.

Process	$k_{0,1}$ $\left[\left(\mathrm{m^3\,kmol^{-1}}\right)^{(n_1-1)}\,\mathrm{s^{-1}}\right]^*$	$\Delta H_{r,1}$ $\left[\frac{\mathrm{kJ}}{\mathrm{mol}}\right]$	$E_{a,1}/R$ [K]	$[\mathrm{A}]_0$ $\left[\frac{\mathrm{kmol}}{\mathrm{m^3}}\right]$	$n_{\mathrm{A},1}$ [−]	$n_{\mathrm{B},1}$ [−]	$\nu_{\mathrm{A},1}$ [−]	$\nu_{\mathrm{B},1}$ [−]
P_1^1	2.76×10^6	-75.0	9525	13.0	1.0	0.0	1.0	1.0
P_2^1	7.65×10^5	-80.0	9525	13.0	1.5	0.0	1.0	2.0
P_3^1	7.00×10^3	-115	9480	13.0	2.0	1.0	2.0	1.0
P_4^1	2.00×10^3	-100	9450	13.0	2.5	1.0	2.0	2.0
P_5^1	2.00×10^2	-25.0	9525	13.0	3.0	1.0	1.0	1.0
P_6^1	2.76×10^6	-130	9525	8.0	1.0	1.0	1.0	1.0

$^*\, n_1 = n_{\mathrm{A},1} + n_{\mathrm{B},1}$

The initial concentration of component B, and the initial temperature of the reactor are held constant for all the above processes. These are set to $[\mathrm{B}]_0 = 21.1\,\mathrm{kmol\ m^{-3}}$ and $T_{R0} = 395\,\mathrm{K}$.

2.3.2. Reaction scheme 2

The process parameters of the second reaction, which is in parallel with the first reaction, are given in Table 2.

Table 2: Process parameters for reaction scheme 2.

Process	$k_{0,2} \times 10^{-3}$ $\left[\left(\mathrm{m^3\,kmol^{-1}}\right)^{(n_2-1)}\,\mathrm{s^{-1}}\right]^*$	$\Delta H_{r,2}$ $\left[\frac{\mathrm{kJ}}{\mathrm{mol}}\right]$	$E_{a,2}/R$ [K]	$[\mathrm{A}]_0$ $\left[\frac{\mathrm{kmol}}{\mathrm{m^3}}\right]$	$n_{\mathrm{A},2}$ [−]	$n_{\mathrm{C},2}$ [−]	$\nu_{\mathrm{A},2}$ [−]	$\nu_{\mathrm{C},2}$ [−]
P_1^2	40.0	-90.0	9400	10.0	1.0	1.0	1.0	2.0
P_2^2	600	-110	9450	10.0	1.0	2.0	1.0	1.0
P_3^2	500	-130	9525	10.0	1.5	1.5	1.0	2.0
P_4^2	400	-250	9350	8.0	2.0	1.0	1.0	1.0
P_5^2	200	-130	9300	11.0	2.0	2.0	1.0	2.0
P_6^2	100	-90.0	9200	8.0	2.0	2.0	1.0	2.0

$^*\, n_2 = n_{\mathrm{A},2} + n_{\mathrm{C},2}$

The initial concentration of components B and C, and the initial temperature of the reactor are held constant for all the above processes. These are set to $[\mathrm{B}]_0 = 8.0\,\mathrm{kmol\ m^{-3}}$, $[\mathrm{C}]_0 = 0.0\,\mathrm{kmol\ m^{-3}}$ and $T_{R0} = 390\,\mathrm{K}$.

2.3.3. Industrial case study: Nitration of toluene

The data used for this reaction network, relevant to industry, are given in Table 3.

Table 3: Process parameters for the nitration of toluene reaction network (Luo and Chang, 1998; Sheats and Strachan, 1978; Chen et al., 2008; Mawardi, 1982).

Reaction	k_0 $\left[\mathrm{m^3\,mol^{-1}\,s^{-1}}\right]$	E_a $\left[\mathrm{kJ\ mol^{-1}}\right]$	ΔH_r $\left[\mathrm{kJ\ mol^{-1}}\right]$	η [−]	κ [−]
(1)	2.00×10^3	76.5	+30.0	1.00	1.00
(2)	109	12.5	-122	2.27	0.293
(3)	67.3	12.5	-122	2.27	0.293
(4)	5.46	12.5	-122	2.27	0.293

This reaction network includes both, an endothermic dissociation reaction (1) and the highly exothermic electrophilic substitution reactions $(2) - (4)$, as shown in Section 2.1.3. Hence, this reaction process gives a good challenge in order to keep the process under control.

The initial concentrations of each reagent are given by:

$$[\mathrm{HNO_3}]_0 = 6.0\,\mathrm{kmol\ m^{-3}} \tag{2.18}$$

$$[\mathrm{H_2SO_4}]_0 = 1.0\,\mathrm{kmol\ m^{-3}} \tag{2.19}$$

$$[\mathrm{C_7H_8}]_0 = 5.5\,\mathrm{kmol\ m^{-3}} \tag{2.20}$$

These initial concentrations are used throughout all case studies for the nitration of toluene.

2.3.4. Physical properties

The changes in viscosity and specific heat capacity of the reaction mixture are estimated according to Hirschfelder et al. (1955), Teja (1983) and Green and Perry (2008):

$$\frac{1}{\rho} = \sum_j y_j/\rho_j \tag{2.21}$$

$$\ln \mu = \sum_j \bar{y}_j \ln \mu_j \tag{2.22}$$

$$C_p = \sum_j y_j\, C_{pj} \tag{2.23}$$

$$\lambda = \sum_j \hat{y}_j\, \lambda_j \tag{2.24}$$

where y_j is the mass fraction, $\bar{y}_j$ is the molar fraction, and $\hat{y}_j$ is the volume fraction of component j.

The physical data used for the equations above are given in Table 4.

Table 4: Physical properties of components A, B, C, D, toluene, mono-nitrotoluene mixtures and a mixture of $HNO_3/H_2SO_4/H_2O$ (Dever et al., 2004; Chen et al., 2008; Bohne et al., 2010; Crittenden et al., 2012).

Physical property [units]	ρ $[\mathrm{kg\,m^{-3}}]$	μ $[\mathrm{Pa\ s^{-1}}]$	C_p $[\mathrm{J\ kg^{-1}\,K^{-1}}]$	λ $[\mathrm{W\ m^{-1}\,K^{-1}}]$
Component				
A	911	1.00×10^{-4}	1100	0.300
B	790	3.00×10^{-4}	950	0.250
C	1200	9.00×10^{-4}	850	0.150
D	1205	2.00×10^{-4}	4200	0.685
Toluene	870	6.00×10^{-4}	1700	0.141
Mono-nitrotoluene mixture	1160	2.00×10^{-4}	1500	0.150
$HNO_3/H_2SO_4/H_2O$ mixture	1430	2.90×10^{-4}	2600	0.540

Since the accurate description of the composition relationships for liquid mixtures is very difficult, Equations (2.21) – (2.24) together with the data in Table 4 are used to determine the physical properties of the reacting mixture.

2.4. Reactor parameters

The chemical reactors' models simulated have a cooling/heating jacket, as can be seen in Figure 1, which controls the reactor temperature by varying the coolant flow rate. A stirrer in each reactor is assumed to be ideal in that all reactor properties are uniform within the reaction mixture. The coolant flow rate is controlled by either a PI controller or by MPC. The reactor properties for each size of reactor are shown in Table 5.

Table 5: Reactor properties used for all processes.

Parameter [units]	V_R $[\mathrm{m^3}]$	V_C $[\mathrm{m^3}]$	A $[\mathrm{m^2}]$	$q_{C,\max}$ $[\mathrm{m^3\,s^{-1}}]$
Process				
$\mathrm{P}_1^1 - \mathrm{P}_3^1$	32	2.0	49	0.060
$\mathrm{P}_1^2 - \mathrm{P}_3^2$	20	1.4	36	0.043
$\mathrm{P}_4^1 - \mathrm{P}_6^1$	8	0.5	20	0.023
$\mathrm{P}_4^2 - \mathrm{P}_6^2$	0.8	0.17	4.2	0.005

The nitration of toluene was carried out in a batch reactor with the same parameters as for processes $\mathrm{P}_1^2 - \mathrm{P}_3^2$.

The heat transfer coefficient U between the reaction mixture and the cooling jacket is evaluated from the flow rate of coolant, as well as the properties of the reaction mixture and the coolant (Sinnot, 2005).

A Proportional-Integral (PI) controller is employed to show the behaviour of thermal runaway reactions. The equation giving the output from a PI controller is given by:

$$q_C(t) = K_p\left(T_R(t) - T_{\mathrm{sp}}(t)\right) + \frac{1}{\tau_I}\int_{t_0}^{t}\left(T_R(t') - T_{\mathrm{sp}}(t')\right)dt' \tag{2.25}$$

where K_p is the proportional, τ_I is the integral parameter, $T_{\mathrm{sp}}(t)$ is the set-point temperature at time t, and t' is a dummy variable for the integral.

As the PI controller is simply used to show the transition of a thermally stable to a thermally unstable system, perfect tuning of the PI controller is not necessary. It is of greater importance in this work to see where the system becomes unstable. To achieve such a behaviour the tuning coefficients were obtained by trial and error, resulting in the parameters given in Table 6.

Table 6: Parameters for PI controller used in case studies.

Parameter	Value
Proportional (P), K_p	10 $\mathrm{m^3\,s^{-1}\,K^{-1}}$
Integral (I), τ_I	1000 $\mathrm{K\,s^2\,m^{-3}}$

All simulations shown in this paper were carried out on an HP EliteDesk 800 G2 Desktop Mini PC with an Intel® Core™ i5-65000 processor with 3.20 GHz and 16.0 GB RAM, running on Windows 7 Enterprise. The system dynamics were simulated using *ode15s* (Shampine et al., 1999) within MATLAB™. MATLAB™ was used due to its simplicity of developing code.

3. Lyapunov exponent method

Many stability criteria are present in literature: Rossi et al. (2015); Melcher (2003); Strozzi and Zaldívar (1999, 1994); Anagnost and Desoer (1991); Barkelew (1959); Semenov (1940); Hurwitz (1895); Routh (1877). As was shown in Kähm and Vassiliadis (2018b) most of these do not apply to non-steady-state systems or do not give reliable results. Hence, Lyapunov exponents are considered which will be shown to give reliable results for such systems. Careful tuning of the parameters involved in this method has to be carried out.

3.1. Derivation

The Lyapunov exponents describe how state variables "drift off" after a large amount of time for an initial small perturbation ϵ. The deviation of the state variables is assumed to follow an exponential profile, which enables to quantify if a stable system is present. A diagram showing the evolution of this deviation is shown in Figure 2.

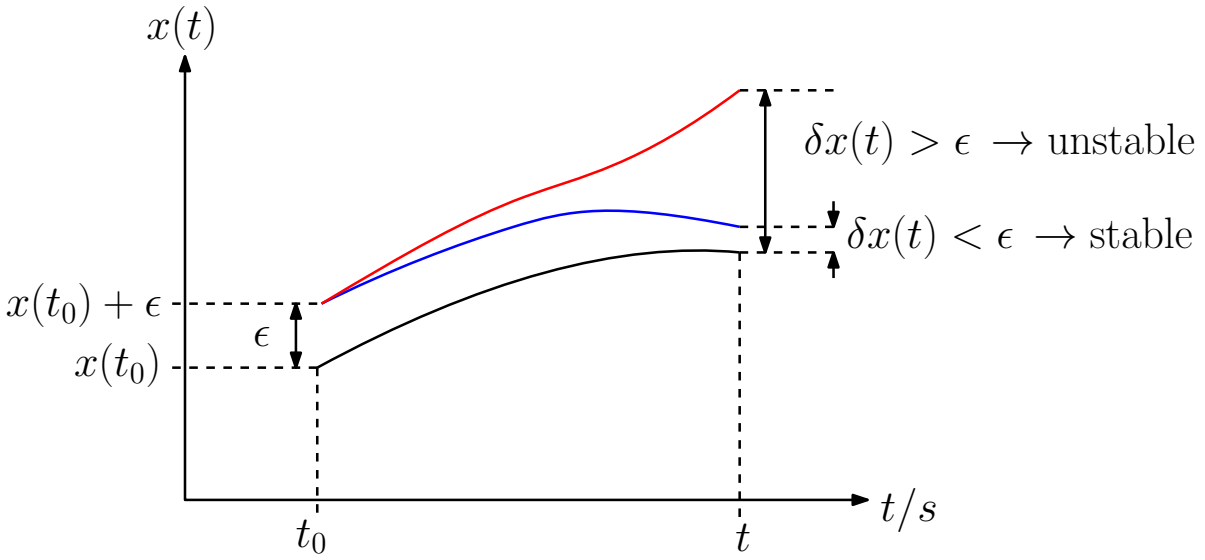

Figure 2: Deviation of an initially perturbed state variable for a stable system (blue line) and an unstable system (red line), respectively.

The following expression quantifies the deviation of an initially perturbed state variable after time t:

$$\epsilon \exp\left(\Lambda\left(x_0\right) t\right) = \left|x\left(t,\, x_0\right) - x\left(t,\, x_0 + \epsilon\right)\right| \tag{3.1}$$

$$\Lambda\left(x_0\right) = \frac{1}{t} \ln\left(\frac{\left|x\left(t,\, x_0\right) - x\left(t,\, x_0 + \epsilon\right)\right|}{\epsilon}\right) \tag{3.2}$$

At the limit of a very small perturbation and infinite time:

$$\Lambda\left(x_0\right) = \lim_{t \to \infty} \left\{ \frac{1}{t} \ln\left(\left|\frac{\delta x\left(t,\, x_0\right)}{\delta x_0}\right|\right) \right\} \tag{3.3}$$

where Λ is known as the *Lyapunov exponent* (Strozzi and Zaldívar, 1994). Numerically, Lyapunov exponents can be evaluated by simulating several systems in parallel, for which each state variable is perturbed initially by an amount $\epsilon = \delta x_0$. Simulating the systems for an infinite amount of time is of course infeasible. Therefore, a large time horizon is chosen instead, which is supposed to give a good approximation of the final value, known as the *local Lyapunov exponent*. This means that at each point in time, a long simulation is carried

out in order to find the local Lyapunov exponent, Λ_{l}, given by:

$$\Lambda_{\mathrm{l}}\left(x_0,\, t\right) = \frac{1}{t_{\mathrm{lyap}}} \ln\left(\left|\frac{\delta x\left(t + t_{\mathrm{lyap}},\, x_0\right)}{\delta x_0}\right|\right) \tag{3.4}$$

The choice of the Lyapunov horizon t_{lyap} in Equation (3.4) is made based on a detailed sensitivity analysis outlined in the sections below. Other methods for evaluating the Lyapunov exponents are available (Melcher, 2003).

Due to the heat generation and removal of the reaction the variables of interest are [A], [B], T_R and T_C. Hence, the local Lyapunov exponents at time t for each state variable are evaluated by:

$$\Lambda_{\mathrm{l},1}\left([\mathrm{A}]_0\,,\, t\right) = \frac{1}{t_{\mathrm{lyap}}} \ln\left(\left|\frac{[\mathrm{A}]\left(t + t_{\mathrm{lyap}}, [\mathrm{A}]_0\right) - [\mathrm{A}]\left(t + t_{\mathrm{lyap}}, [\mathrm{A}]_0 + \epsilon\right)}{\epsilon}\right|\right) \tag{3.5}$$

$$\Lambda_{\mathrm{l},2}\left([\mathrm{B}]_0\,,\, t\right) = \frac{1}{t_{\mathrm{lyap}}} \ln\left(\left|\frac{[\mathrm{B}]\left(t + t_{\mathrm{lyap}}, [\mathrm{B}]_0\right) - [\mathrm{B}]\left(t + t_{\mathrm{lyap}}, [\mathrm{B}]_0 + \epsilon\right)}{\epsilon}\right|\right) \tag{3.6}$$

$$\Lambda_{\mathrm{l},3}\left(T_{R,0},\, t\right) = \frac{1}{t_{\mathrm{lyap}}} \ln\left(\left|\frac{T_R\left(t + t_{\mathrm{lyap}}, T_{R,0}\right) - T_R\left(t + t_{\mathrm{lyap}}, T_{R,0} + \epsilon\right)}{\epsilon}\right|\right) \tag{3.7}$$

$$\Lambda_{\mathrm{l},4}\left(T_{C,0},\, t\right) = \frac{1}{t_{\mathrm{lyap}}} \ln\left(\left|\frac{T_C\left(t + t_{\mathrm{lyap}}, T_{C,0}\right) - T_C\left(t + t_{\mathrm{lyap}}, T_{C,0} + \epsilon\right)}{\epsilon}\right|\right) \tag{3.8}$$

The evaluation of the Lyapunov exponents requires a particular value of the control variable, in this case the coolant flow rate. For both, PI and MPC controlled systems 95% cooling capacity is assumed. Detailed sensitivity analyses on choosing values for the initial perturbation, ϵ and the Lyapunov time frame, t_{lyap}, are carried out in the following sections. A detailed description of the MPC scheme used is given in Section 4.

3.2. Sensitivity analysis for initial perturbation ϵ

To show how the choice of ϵ affects the results obtained for the Lyapunov exponents, a sensitivity analysis on ϵ is carried out for reaction schemes 1 and 2. For values of $\epsilon = 10^0$, 10^{-1}, 10^{-2}, 10^{-3}, 10^{-4} the Lyapunov exponent profiles are evaluated for process P_1^1. The temperature profile for this process is shown in Figure 3.

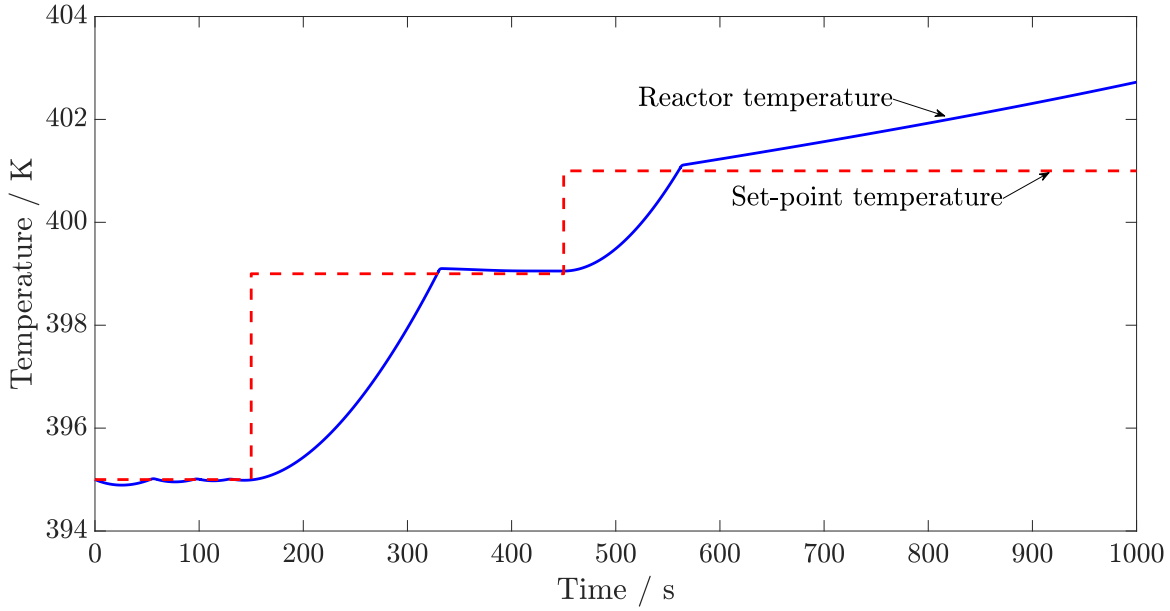

Figure 3: Temperature profile of process P_1^1.

The errors for each Lyapunov exponent with respect to the values obtained when setting $\epsilon = 10^{-5}$ and $t_{\text{lyap}} = 5000$ s as a reference are computed and shown in Figures 4−7.

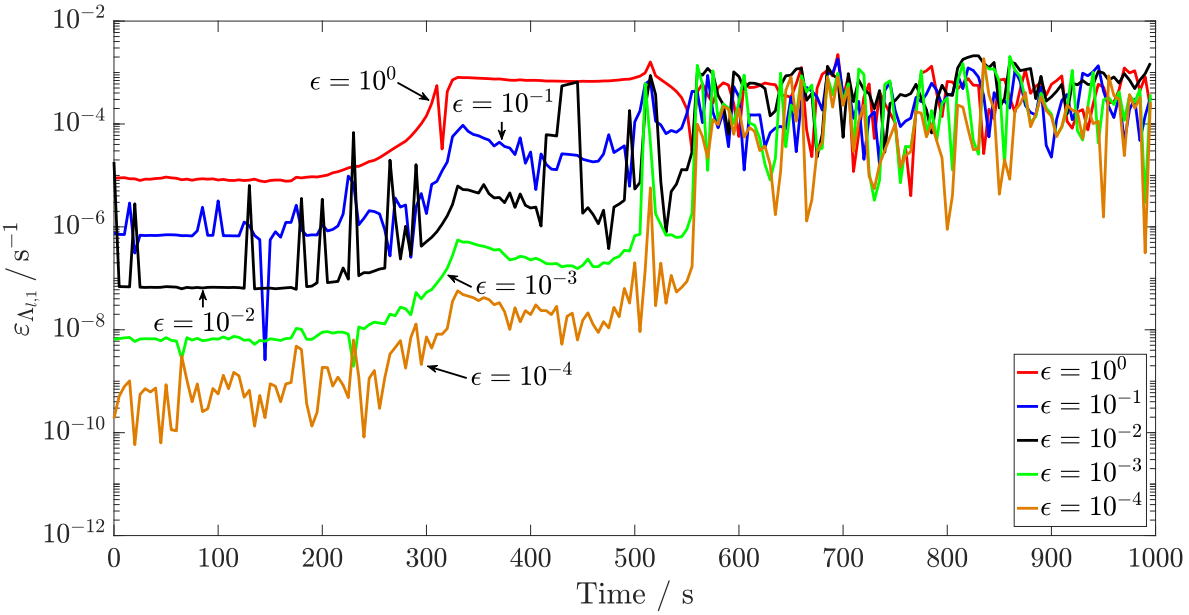

Figure 4: Errors ε obtained for the Lyapunov exponents with respect to state variable [A], $\Lambda_{l,1}$, with changes in the initial perturbation ϵ for process P_1^1.

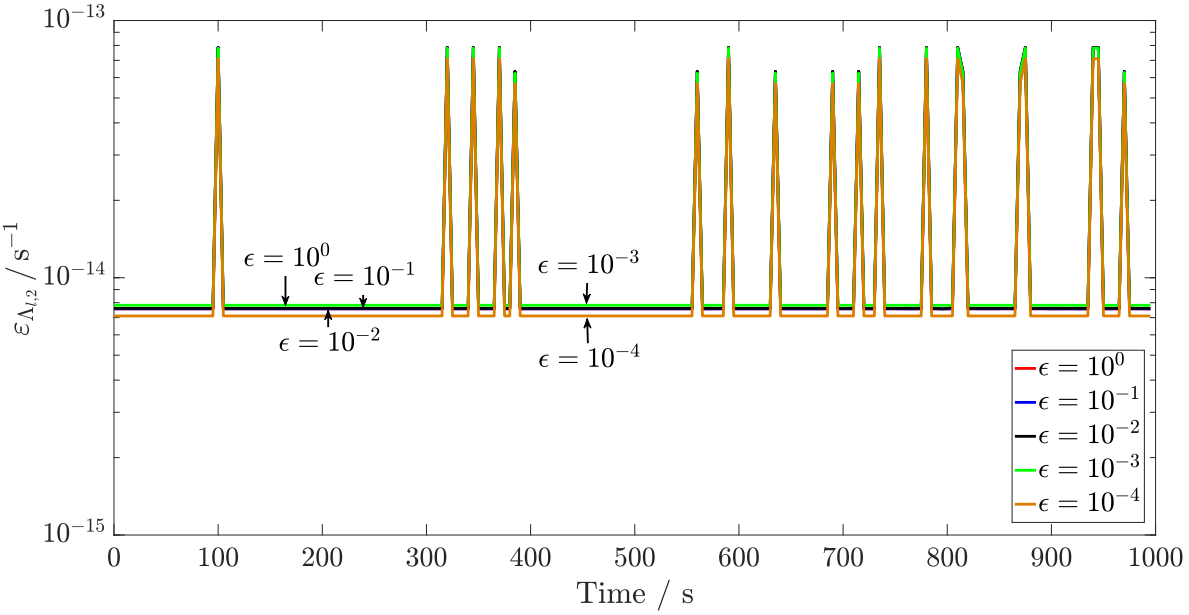

Figure 5: Errors ε obtained for the Lyapunov exponents with respect to state variable [B], $\Lambda_{l,2}$, with changes in the initial perturbation ϵ for process P_1^1.

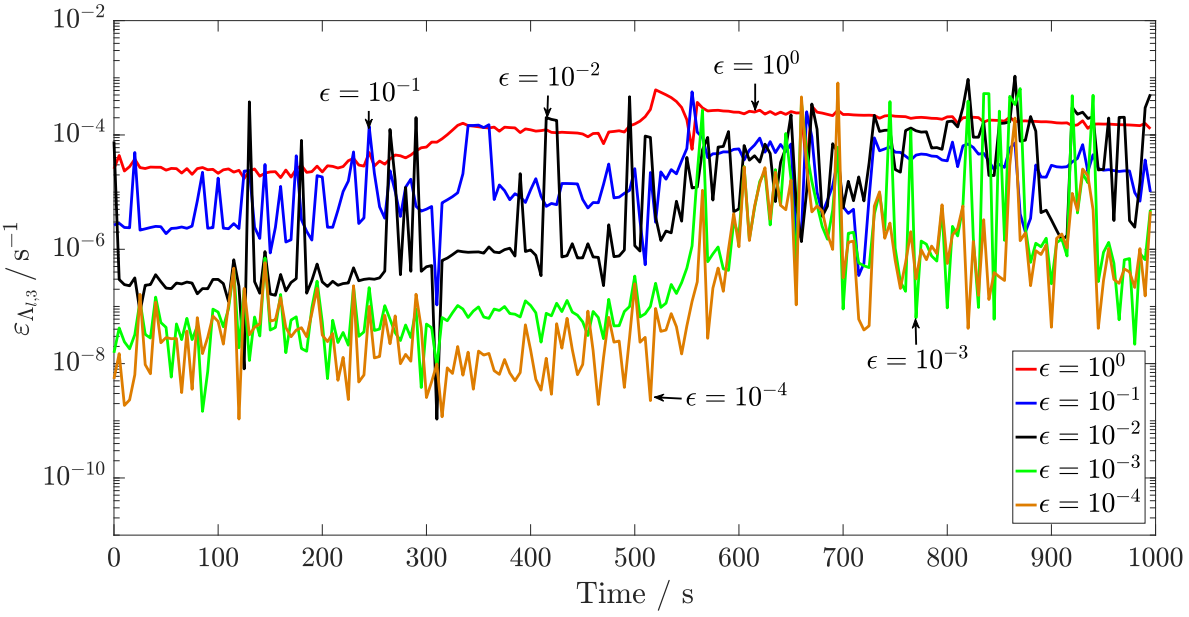

Figure 6: Errors ε obtained for the Lyapunov exponents with respect to state variable T_R, $\Lambda_{l,3}$, with changes in the initial perturbation ϵ for process P_1^1.

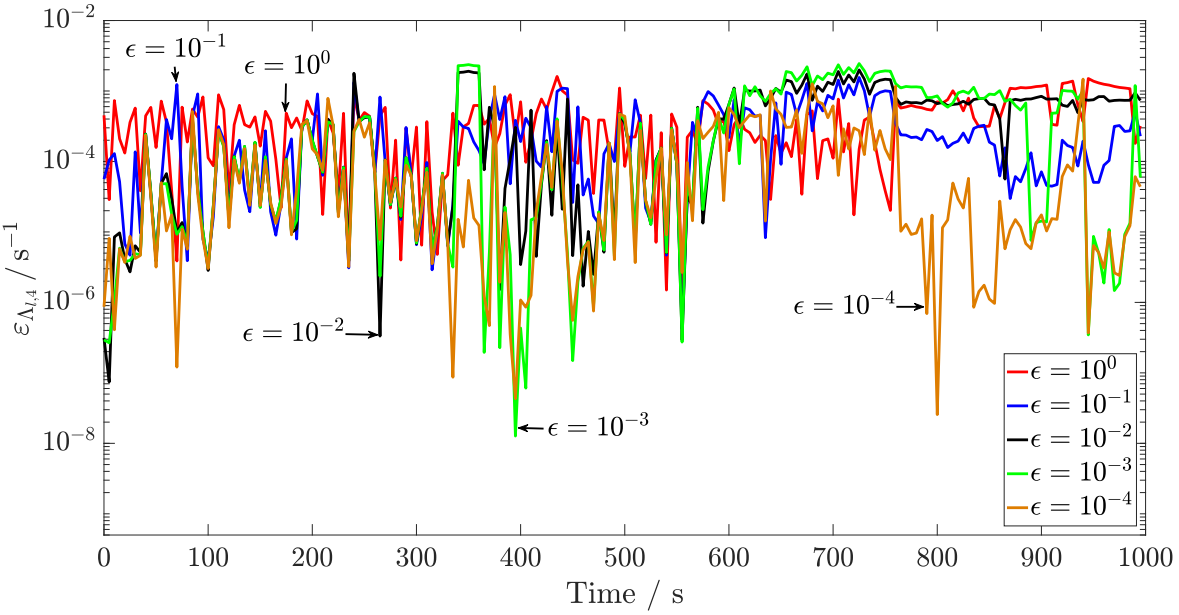

Figure 7: Errors ε obtained for the Lyapunov exponents with respect to state variable T_C, $\Lambda_{l,4}$, with changes in the initial perturbation ϵ for process P_1^1.

The errors obtained for the Lyapunov exponents when using various initial perturbations are similar, and have a maximum value of approximately 10^{-3}. This is a relatively large error, but the relative size compared to the magnitude of the Lyapunov exponents is of greater importance. For the second Lyapunov exponent with respect to the concentration of B the errors are close to zero. This is the case because the reaction kinetics for process P_1^1 do not depend on component B and therefore the initial perturbation of the concentration of B has no effect. The values obtained are more likely due to numerical effects and therefore of order 10^{-14}.

The smaller the initial perturbation, the more prone the stability detection is to fluctuations in the final values obtained. Since all profiles mostly follow the same trend, an optimal initial perturbation of $\epsilon = 10^{-3}$ is chosen.

No additional information can be obtained by reducing the size of the initial perturbation epsilon, as this can result in wrong predictions of the thermal stability due to numerical inaccuracies.

3.3. Determination of reliable time horizon t_{lyap}

To show how the choice of t_{lyap} affects the results obtained for the Lyapunov exponents, a sensitivity analysis on t_{lyap} is carried out. For values of $t_{\mathrm{lyap}} = 1000$, 2500, 5000, 10^4, and 5×10^4 s the Lyapunov exponent profiles are evaluated for process P_1^1, the temperature profile of which is shown in Figure 3. For clarity, only the analysis of process P_1^1 is presented here,

as for all other processes the similar results are obtained. The respective profiles for each Lyapunov exponent with respect to the values obtained when $\epsilon = 10^{-3}$ are computed and shown in Figures 8−11.

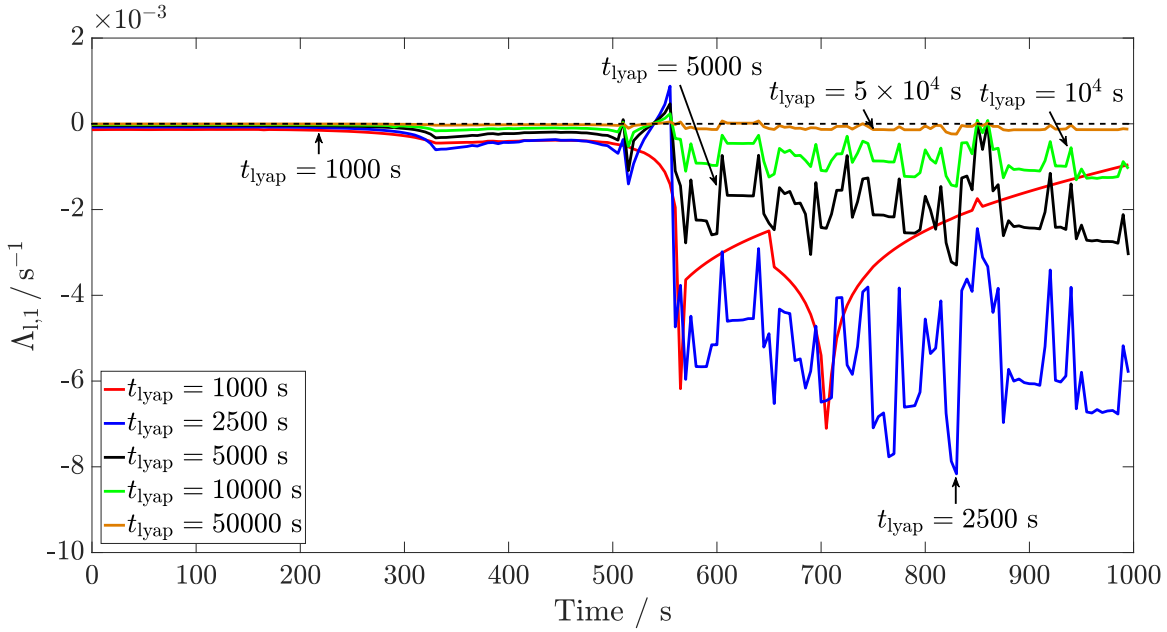

Figure 8: Lyapunov exponent profiles with respect to state variable [A], $\Lambda_{l,1}$, with various setting for the Lyapunov time frame t_{lyap} for process P_1^1.

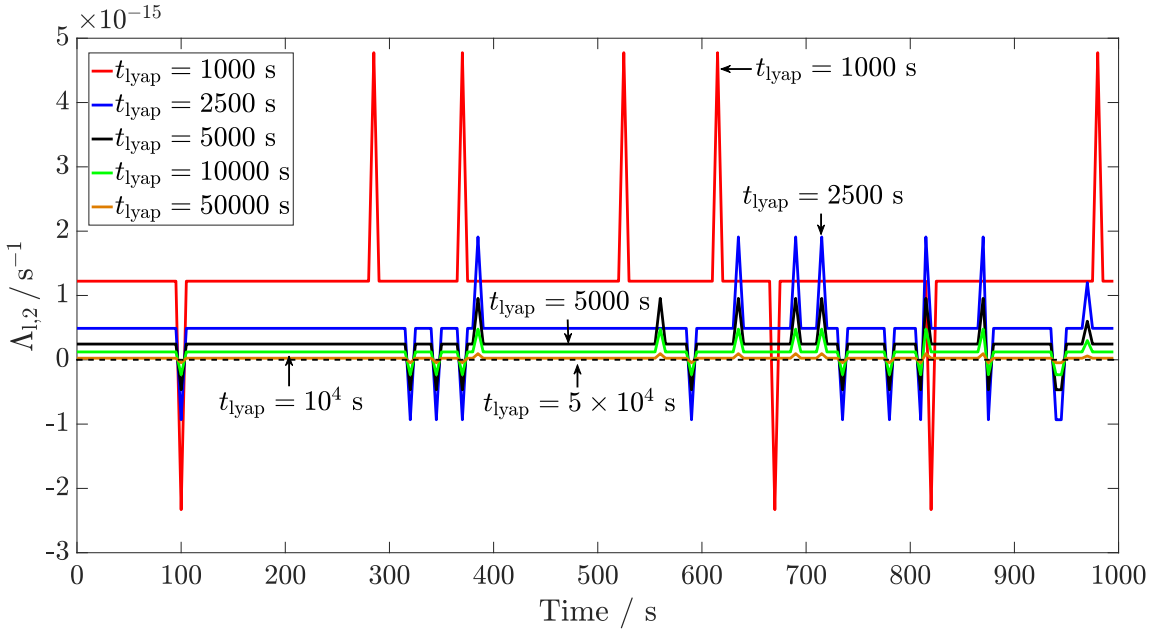

Figure 9: Lyapunov exponent profiles with respect to state variable [B], $\Lambda_{l,2}$, with various setting for the Lyapunov time frame t_{lyap} for process P_1^1.

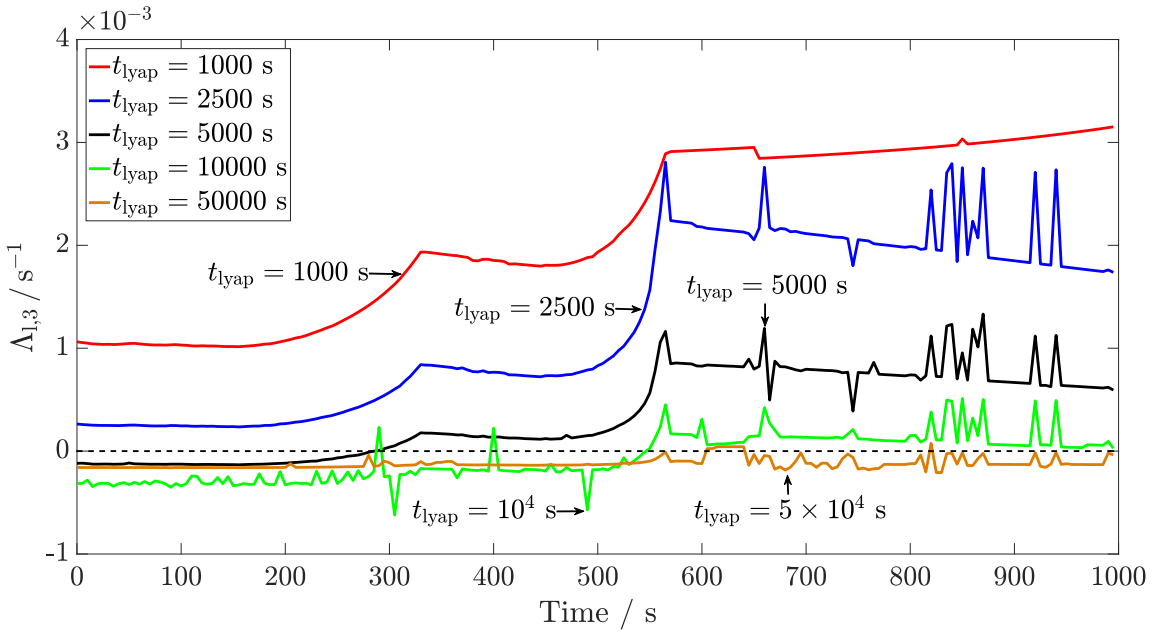

Figure 10: Lyapunov exponent profiles with respect to state variable T_R, $\Lambda_{\mathrm{l},3}$, with various setting for the Lyapunov time frame t_{lyap} for process P_1^1.

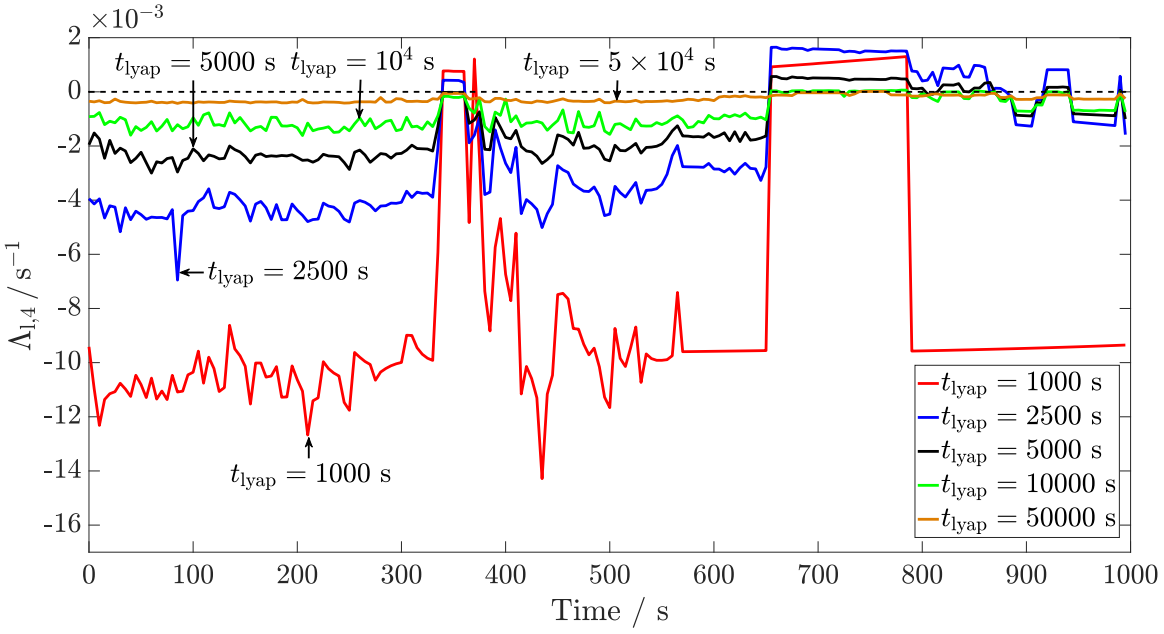

Figure 11: Lyapunov exponent profiles with respect to state variable T_C, $\Lambda_{\mathrm{l},4}$, with various setting for the Lyapunov time frame t_{lyap} for process P_1^1.

In Figures 8, 10 and 11 it can be seen that different Lyapunov horizons t_{lyap} lead to different predictions of system stability. For the Lyapunov exponents with respect to the concentration of B, shown in Figure 9, the values obtained are close to zero (of the order of 10^{-14}),

as component B has no effect on the reaction kinetics. Furthermore it can be seen that the most useful Lyapunov exponent relates to the temperature of the system: for stability of batch reactors the thermal stability is of interest. Hence the Lyapunov exponent with respect to the temperature gives the best indication of system stability. The Lyapunov exponents with respect to concentration [A] are initially negative, only becoming positive in a sharp manner when the system starts to become unstable at $t \approx 500$ s. Directly after the sharp increase, the values for $\Lambda_{l,1}$ become negative again, although the thermal runaway is starting. Therefore using $\Lambda_{l,1}$ as the main indicator of instability is unreliable. Nevertheless valuable information can be obtained at the point where the system becomes unstable.

For the Lyapunov exponent with respect to the coolant temperature, $\Lambda_{l,4}$, no valuable information can be extracted as the values of the exponents do not correspond well to the temperature profile of the thermal runaway. This can be seen in Figure 11 as the regions in which $\Lambda_{l,4} > 0$ do not coincide with the loss of stability after $t = 550$ s given by the temperature profile within the reactor, which is shown in Figure 3.

The Lyapunov exponent with respect to the system temperature, $\Lambda_{l,3}$, gives a good estimate of the system stability when using a Lyapunov time frame of $t_{\text{lyap}} = 5000$ s. At time $t = 300$ s a thermal runaway is predicted. At this point in time the temperature is 2 K below the loss of stability. Using a Lyapunov time frame of $t_{\text{lyap}} = 10^4$ s predicts the stability correctly at $t = 550$ s. This time frame is twice the size of $t_{\text{lyap}} = 5000$ s and as such will result in higher computational cost. As it is required to have a stability criterion with low computational cost, the optimal time frame of $t_{\text{lyap}} = 5000$ s is chosen for further applications. The conservative nature of the stability estimate is in the best interest for control schemes, as therefore the boundary of stability is never crossed, giving stable operation.

The Lyapunov exponents due to the concentrations do not give a clear indication of when the system becomes unstable. Nevertheless, for more complex systems, the effect due to concentration will not be ignored. As can be seen in Figure 8 there is a spike in the Lyapunov exponent with respect to the concentration of A at approximately 500 s, which suggests that valuable information can still be present. Therefore, for the PI control case studies following this section, only Λ_3 corresponding to the reactor temperature is plotted. In the Model Predictive Control (MPC) case studies in Section 4 the Lyapunov exponents with respect to concentrations as well as reactor temperature are included as constraints in the MPC schemes.

3.4. Verification of Lyapunov exponents for system stability

The verification of Lyapunov exponents, evaluated with the optimal values for ϵ and t_{lyap} found above, with respect to the point of loss of stability is carried out for reaction schemes 1 and 2. Similarly to the results shown in Kähm and Vassiliadis (2018a), once it is shown

that Lyapunov exponents give a reliable prediction of system stability, this criterion can be applied to advanced control schemes such as MPC.

3.4.1. Reaction scheme 1

Detecting the stability of batch processes is the main task of the Lyapunov exponents in this work. Hence an initially stable process with PI control will artificially be made unstable with step changes in the set point temperature. The first step change in set-point temperature leads to a still controllable system, while the second step change causes the system to enter the unstable regime. Hence a clear transition form stable to unstable operation can be observed to prove Lyapunov exponents are reliable at predicting system stability. The temperature profiles for processes $P_1^1 - P_6^1$ are shown in Figure 12.

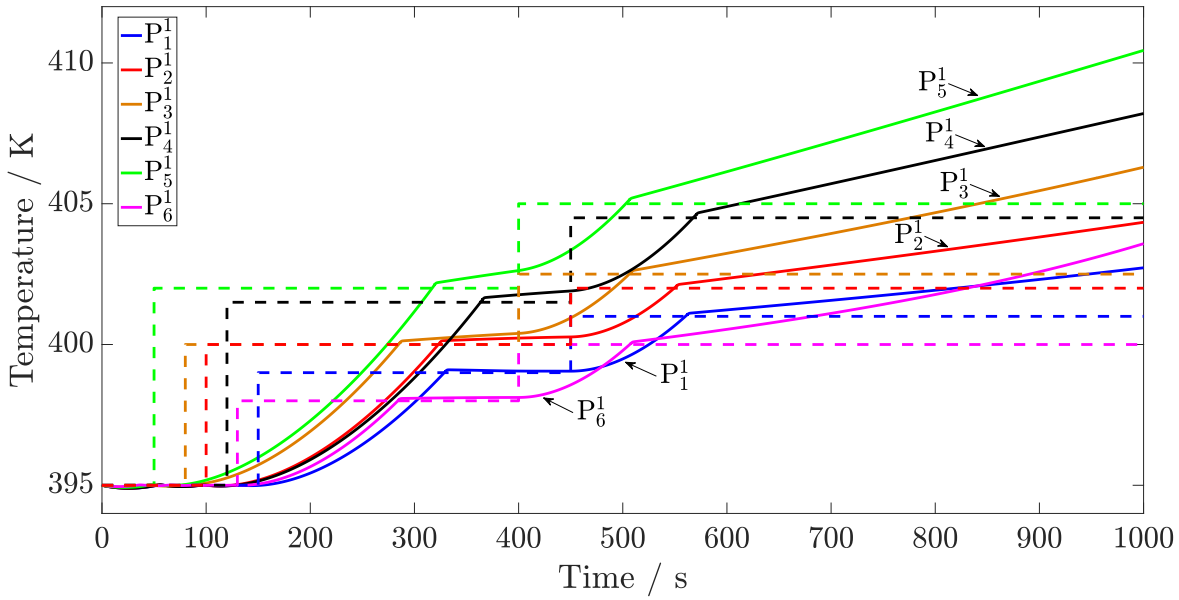

Figure 12: Temperature profiles for processes $P_1^1 - P_6^1$ as solid lines. Temperature set-points are given by dashed lines with respective colour.

The Lyapunov exponents for the temperature of the batch reactor contents, $\Lambda_{l,3}$, with respect to the above temperature profiles are shown in Figure 13.

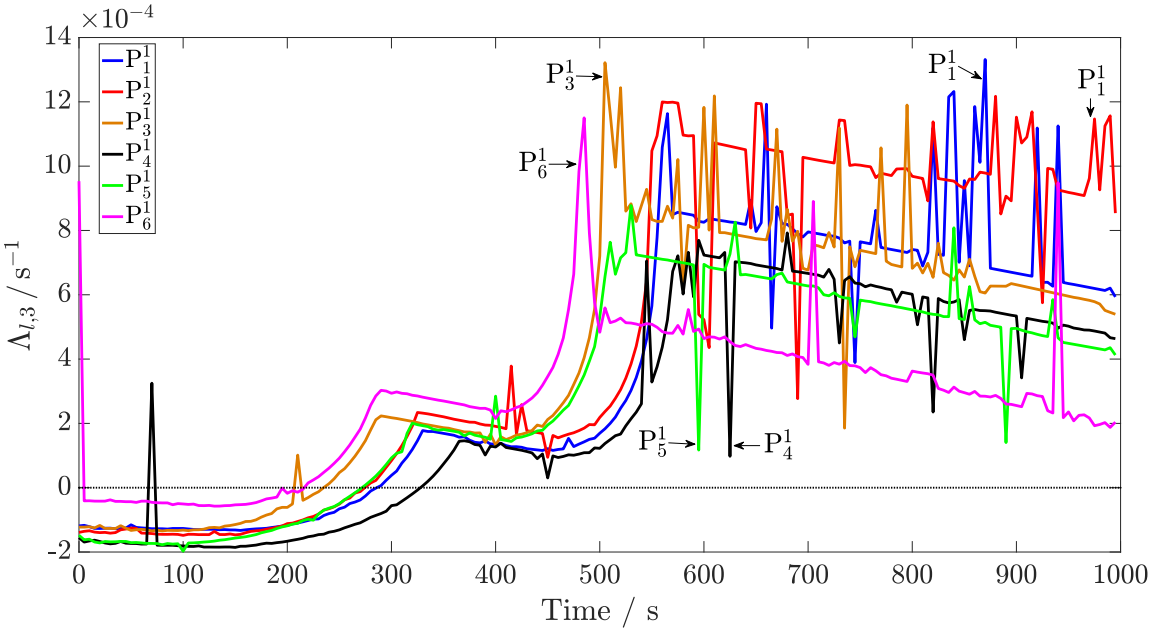

Figure 13: Lyapunov exponent profiles with respect to reactor temperature, $\Lambda_{l,3}$, for processes $\mathrm{P}_1^1 - \mathrm{P}_6^1$. The dotted line indicates zero, giving the switch-over from stable to unstable operation.

As can be seen in Figure 13 a thermal runaway of the reactor system is predicted before it occurs in Figure 12. For each system the instability is predicted approximately 2 K before, hence giving a conservative stability measure.

From these results it can be seen that for single reactions, as given in reaction scheme 1, Lyapunov exponents are a reliable and conservative stability measure. In the following section it is shown that this criterion can also be used for more complex reaction schemes.

The conservative nature comes from the predictive property as the perturbed state profiles have to be simulated for a certain Lyapunov time frame t_{lyap}. As was shown in Kähm and Vassiliadis (2018b) other stability criteria in literature result in extremely conservative processes if embedded in an MPC scheme. Lyapunov exponents do not give overly conservative estimates of stability as the processes to which they are applied are still intensified.

3.4.2. Reaction scheme 2

In this section it is shown that the use of Lyapunov exponents is not only reliable for single reactions, but also for series reactions. The temperature profiles of processes $\mathrm{P}_1^2 - \mathrm{P}_6^2$, the parameters of which are shown in Table 2, are shown in Figure 14.

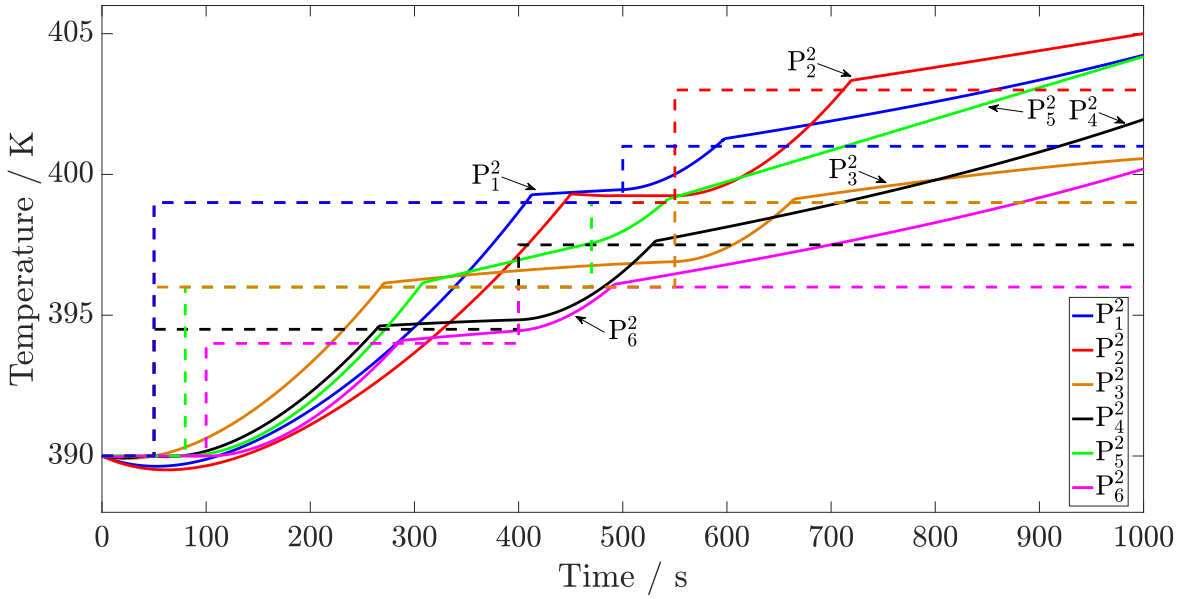

Figure 14: Temperature profiles for processes $P_1^2 - P_6^2$ as solid lines. Temperature set-points are given by dashed lines with respective colour.

352 The respective Lyapunov exponent profiles with respect to reactor temperature, $\Lambda_{l,3}$, are
353 given in Figure 15.

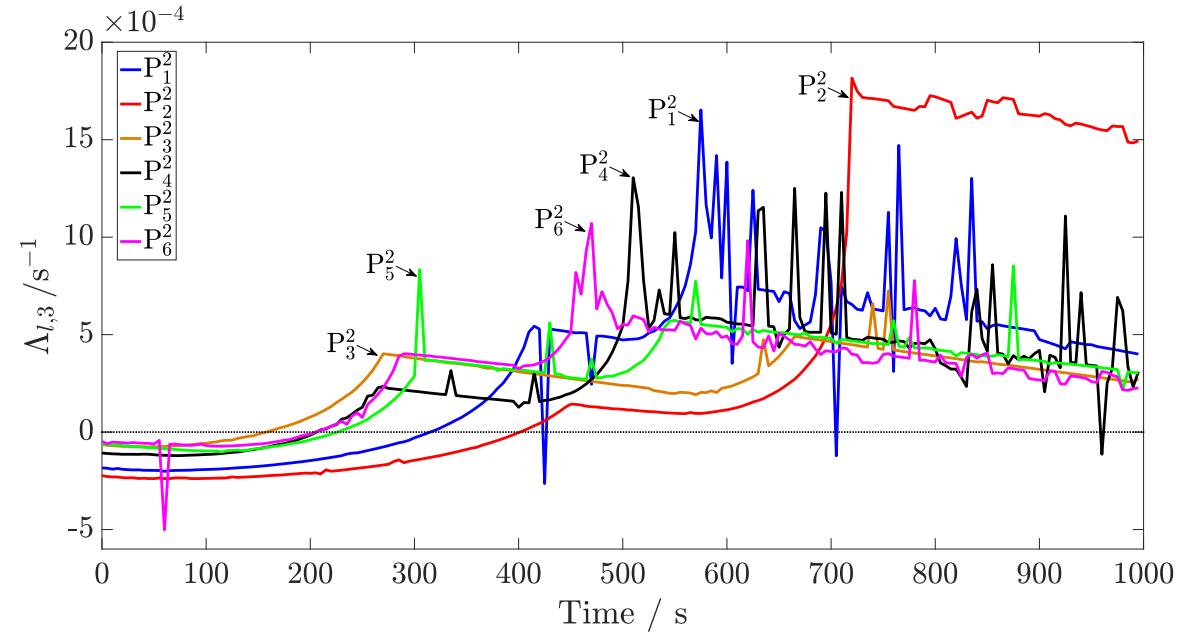

Figure 15: Lyapunov exponent profiles with respect to reactor temperature, $\Lambda_{l,3}$, for processes $P_1^2 - P_6^2$. The dotted line indicates zero, giving the switch-over from stable to unstable operation.

354 As was observed for reaction scheme 1, a conservative and reliable stability measure is

obtained for reaction scheme 2. The value of the Lyapunov exponent with respect to reactor temperature, $\Lambda_{l,3}$, becomes positive before a thermal runaway occurs. This gives advanced control schemes enough time to react to potential disturbances in the system. The thermal runaways are predicted 2-3 K before the thermal runaways occur, giving some robustness in case of deviations in temperature measurements.

The case studies shown for reactions schemes 1 and 2 show that using Lyapunov exponents for measuring system stability is a feasible method. The implementation of Lyapunov exponents within MPC schemes is discussed in detail in the following section.

4. Model Predictive Control with Lyapunov Exponents

In this section the structure of common MPC schemes, as well as the scheme embedding Lyapunov exponents as presented in Kähm and Vassiliadis (2018a), is outlined. The basic concepts of MPC are described and the reformulation of the problem for such control schemes is shown. The computational time required for such a control scheme is analysed for cases where the respective batch reaction is intensified, giving the smallest possible time to complete the reaction. Furthermore, the improved control profiles and thermal stability of the processes controlled similar to Kähm and Vassiliadis (2018a) are outlined.

4.1. Model Predictive Control Structure

Model Predictive Control (MPC) started to be vastly implemented in industry in the 1980s as an alternative to the then (and now) commonly used PID control (Lee, 1994, 2011). The advantage of MPC over PID controllers is the capability of optimising a system during operation, whilst considering system constraints and nonlinear system dynamics (Chuong La et al., 2017; Anucha et al., 2015; Mayne, 2014). Constraints cannot be included in PID control which leads to saturation of control valves or exceeding certain criteria for the process, *e.g.* maximum allowable temperatures.

MPC is capable of using a process model to continuously carry out a specified optimisation of control variables, also called inputs, in order to achieve that particular goal (Haber et al., 2011). For this purpose a method called "receding horizon" control is employed, which is described in detail in Rawlings and Mayne (2015) and Christofides et al. (2011).

In this approach of process control the process model is used to predict how the system will behave to certain input values. It is desired to reach a given reference trajectory as quickly as possible, while satisfying all constraints. The inputs are usually split into several control steps during which the value of the input does not change (piecewise constant) over a control horizon t_c (Akpan and Hassapis, 2011). In order to make sure a solution is obtained which converges to the desired reference trajectory, a prediction horizon t_p is included, for

which the system is simulated with the control inputs found from the optimisation. As is the case for PID control, tuning is an essential part for MPC: the number of control steps, the control horizon t_c as well as prediction horizon t_p have to be adjusted until satisfactory control is achieved (Christofides et al., 2011). Except for some special cases, an extension of t_p will lead to more stable control (Haber et al., 2011).

The optimisation problem for the MPC implementation at time $t^{(i)}$, which is the i^{th} step, is formulated in the following way (Rawlings and Mayne, 2015; Charitopoulos and Dua, 2016):

$$\min_{q_C(t)} \Phi^{(i)}\left(x\left(t\right),\, q_C\left(t\right)\right) = \int_{t_0^{(i)}}^{t_f^{(i)}} \left(T_R - T_{\text{sp}}\right)^2 \mathrm{d}t \tag{4.1a}$$

subject to:

$$0 = h\left(x\left(t\right),\, q_C\left(t\right),\, t\right) \tag{4.1b}$$

$$T_R \leq T_{\text{chem}} \tag{4.1c}$$

$$\left|q_C^{(i)} - q_C^{(i-1)}\right| \leq \delta q_C \tag{4.1d}$$

$$\Lambda_{\text{l},1},\, \Lambda_{\text{l},2},\, \Lambda_{\text{l},3} \leq 0 \tag{4.1e}$$

$$0 \leq q_C^{(i)} \leq q_{C,\max} \tag{4.1f}$$

$$t_0 \leq t \leq t_f \tag{4.1g}$$

where $\Phi^{(i)}$ is the objective function of the optimisation, and $x\left(t\right)$ are the state variables of the system, $h\left(x\left(t\right),\, q_C\left(t\right),\, t\right)$ are the equations giving the physical properties, $t_0^{(i)}$ and $t_f^{(i)}$ are the initial time and final time of the simulation at step i, respectively, and T_{chem} is the chemical stability temperature. The change in coolant flow rate between steps i and $i-1$, $q_C^{(i)} - q_C^{(i-1)}$, is limited to at most equal to δq_C, which is set to $\delta q_C = 0.05\, q_{\max}$. $\Lambda_{\text{l},1}$, $\Lambda_{\text{l},2}$, $\Lambda_{\text{l},3}$ are the local Lyapunov exponents with respect to concentration of components A and B, and the system temperature, respectively, which are incorporated into the MPC scheme for improved stability of the resulting process. The problem given in Equations (4.1a) - (4.1g) is solved using the SQP optimisation algorithm (Nocedal and Wright, 2006) within *fmincon* in MATLAB$^{\text{TM}}$. The implementation of the optimal control problem solution with the nonlinear MPC framework was sequential.

Three different MPC schemes are considered in this section:

1. MPC with Lyapunov exponents
2. MPC with constant set-point temperature
3. MPC with extended prediction horizon

The first scheme is the implementation discussed above and in Kähm and Vassiliadis (2018a). This MPC scheme uses a control horizon of $t_c = 40$ s with four control increments, each with length of 10 s, and no extended prediction horizon. The Lyapunov horizon is set to $t_{\text{lyap}} = 5000$ s with an initial perturbation of $\epsilon = 10^{-3}$, as derived from the sensitivity analysis in Section 3. For the evaluation of the Lyapunov exponents the cooling valve position after the control horizon is assumed to be 95%, as was done for all Lyapunov exponent evaluations before in this work.

The second scheme is often found in industry: rather than increasing the temperature set-point during a process, it is easier to keep the reaction temperature constant in order to ensure stability of operation. This MPC scheme uses a control horizon of $t_c = 30$ s with three control increments, each with length of 10 s, and no extended prediction horizon.

The third scheme is an alternative to using stability criteria altogether: as the prediction horizon of the MPC formulation is extended, the optimisation algorithm should be able to find control inputs which keep the system close to the desired temperature set-point and within the defined constraints. The control horizon for this scheme is set to $t_c = 50$ s with five control increments, each with length of 10 s, and a prediction horizon of $t_p = 10000$ s.

These three schemes are compared with respect to reliability of control and computational cost.

4.2. Computational time of batch processes with Lyapunov exponents

In this section the three MPC schemes described above are implemented to intensify reaction schemes 1 and 2, as well as the nitration of toluene, outlined in Section 2.1. Each MPC scheme is analysed in terms of computational time and stability to achieve an intensification of the respective batch reaction.

4.2.1. Intensification of reaction scheme 1

In this section the three MPC schemes discussed above are compared. The objective is to increase the reaction temperature to a maximum of $T_{\text{chem}} = 470$ K, whilst keeping the process under control. The temperature profiles for each MPC implementation applied to processes P_1^1 and P_2^1 are shown in Figure 16.

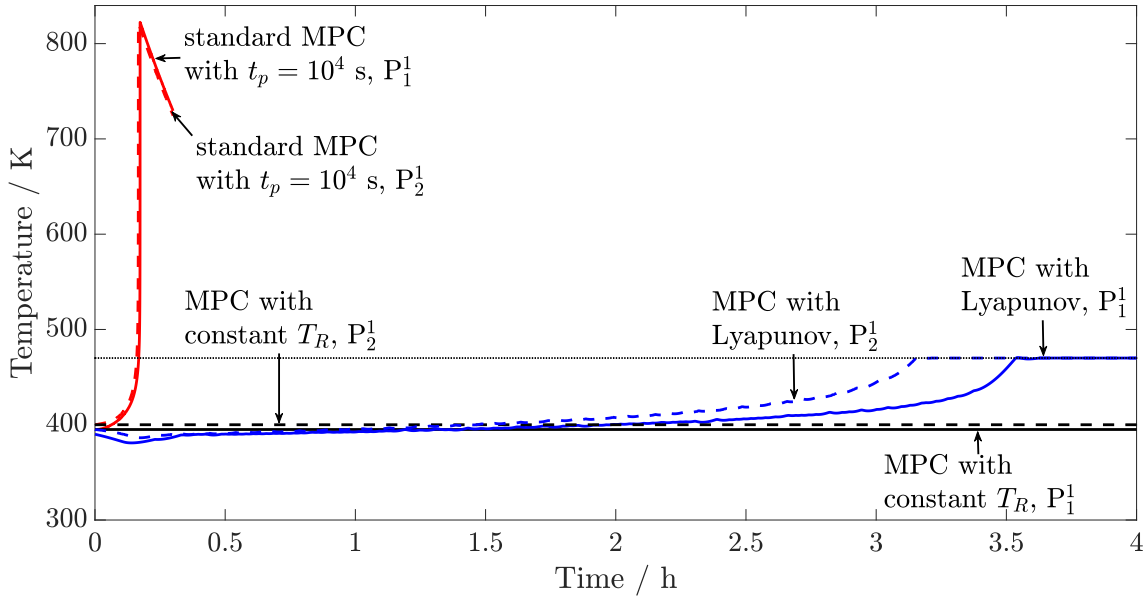

Figure 16: Temperature profiles for each MPC scheme applied to processes P_1^1 and P_2^1. Solid lines correspond to process P_1^1, dashed lines to P_2^1. The dotted line represents the maximum allowable temperature of $T_{\text{chem}} = 470\,\text{K}$.

The MPC scheme incorporating Lyapunov exponents results in stable operation of the system. The reactor temperature increases in a steady manner until the maximum temperature is reached, without violating this constraint.

A constant temperature set-point for the standard MPC implementation gives steady operation for processes P_1^1 and P_2^1. No thermal runaway occurs for these processes, as the temperature is not increased during the operation.

The standard nonlinear MPC scheme using an extended prediction horizon does not yield stable operation. This is observed due to the thermal runaway peaks reaching a maximum temperature of $T_R = 820$ K for both process P_1^1 and process P_2^1, therefore exceeding the maximum allowable temperature.

The coolant valve positions for processes P_1^1 and P_2^1 controlled by each MPC scheme are shown in Figure 17.

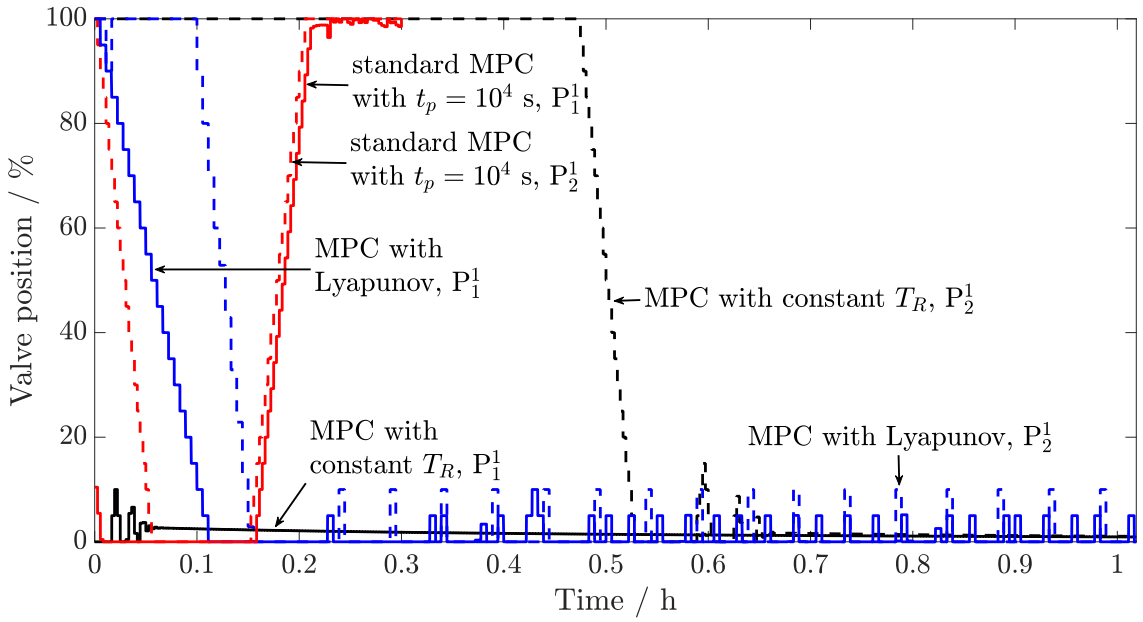

Figure 17: Cooling valve position for each MPC scheme applied to processes P_1^1 and P_2^1. Solid lines correspond to process P_1^1, dashed lines to P_2^1.

In Figure 17 it is seen that the coolant valve position for MPC scheme 1 high cooling intensity is present at first for processes P_1^1 and P_2^1. As stable operation is reached, the extent of cooling is reduced hence intensifying the process. As the temperature increases, cooling is activated from time to time in order to keep the process stable.

Keeping a constant reactor temperature for processes P_1^1 and P_2^1 is achieved with MPC scheme 2 by slowly reducing the cooling capacity, since as the concentration is depleted the reaction rate decreases, and hence the rate of heat generation of the reactor decreases also.

MPC scheme 3 initially starts with low cooling capacity in contrast to MPC schemes 1 and 2. This control is obtained as the prediction horizon is not large enough to recognise that the process will enter an unstable region. Therefore no cooling is present until the standard MPC scheme recognises that the maximum allowable temperature constraint cannot be satisfied within the prediction horizon, upon which the cooling is increased at the maximum allowable rate.

The temperature profiles for each MPC implementation applied to processes P_3^1 and P_4^1 are shown in Figure 24.

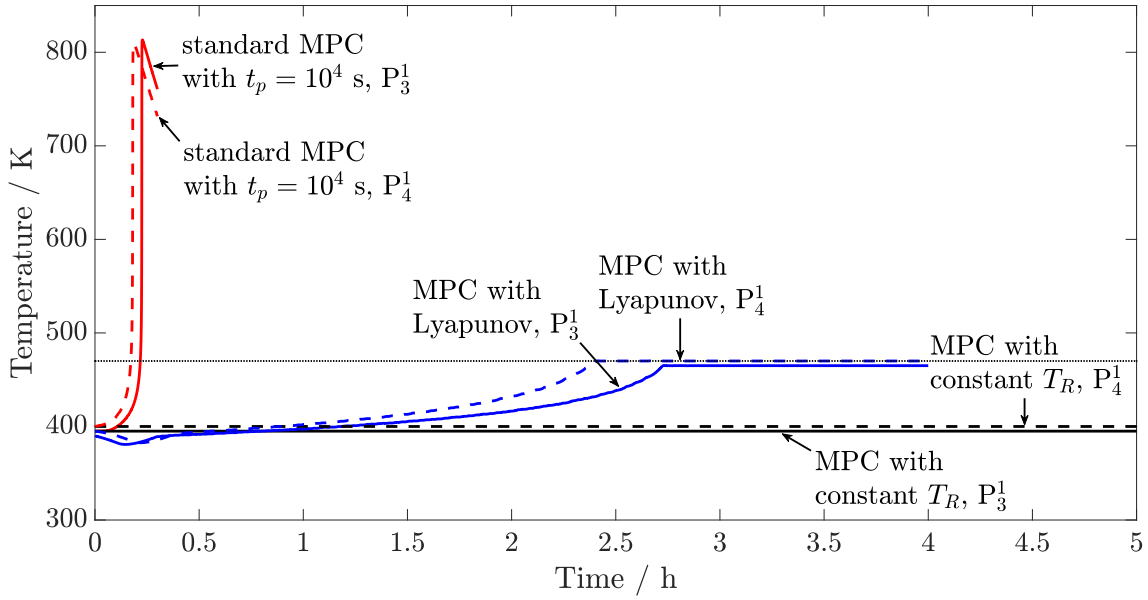

Figure 18: Temperature profiles for each MPC scheme applied to processes P_3^1 and P_4^1. Solid lines correspond to process P_3^1, dashed lines to P_4^1. The dotted line represents the maximum allowable temperature of $T_{\text{chem}} = 470\,\text{K}$.

The MPC scheme using Lyapunov exponents of the reactor temperature results in stable operation of processes P_3^1 and P_4^1. The reactor temperature is continuously increased, but always kept below the chemical temperature constraint of $T_{\text{chem}} = 470\,\text{K}$.

A constant temperature set-point for processes P_3^1 and P_4^1 results in stable operation throughout each process. Due to the constant temperature it is expected that the rate of conversion for this control strategy is slower than for the other MPC schemes. Since MPC schemes 1 and 2 result in stable operation, the computational time of each will be of interest.

Thermal runaways are observed for the processes using a standard MPC scheme with an extended prediction horizon. The peak temperatures for processes P_3^1 and P_4^1 are both at approximately $T_R = 800$ K, exceeding the maximum allowable temperature. Therefore, this type of MPC strategy does not yield satisfactory system control.

The temperature profiles for each MPC implementation applied to processes P_5^1 and P_6^1 are shown in Figure 19.

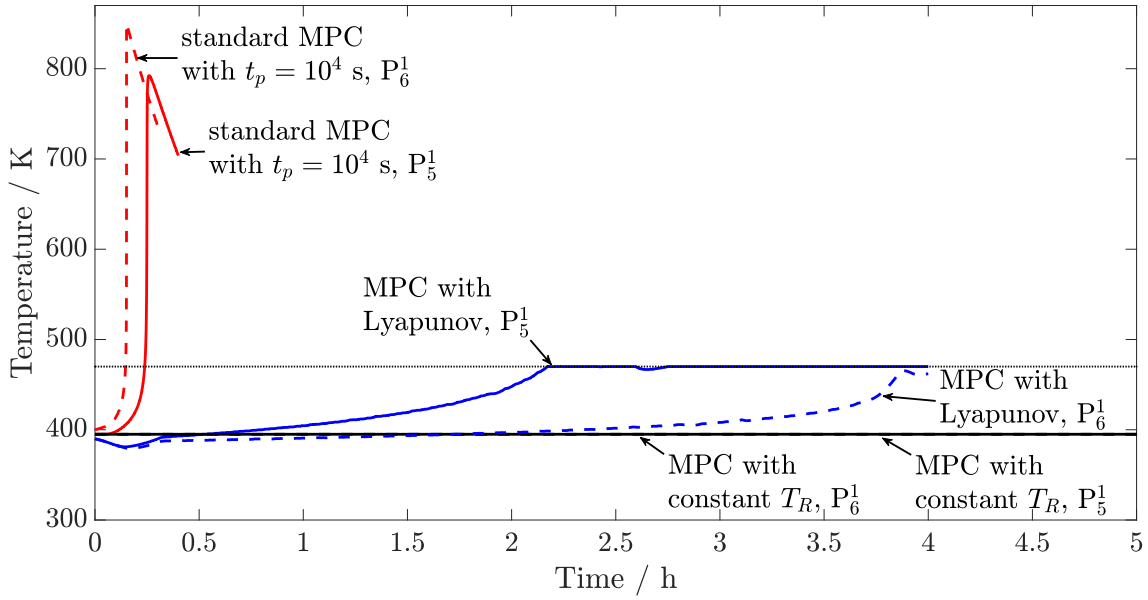

Figure 19: Temperature profiles for each MPC scheme applied to processes P_5^1 and P_6^1. Solid lines correspond to process P_5^1, dashed lines to P_6^1. The dotted line represents the maximum allowable temperature of $T_{\text{chem}} = 470\,\text{K}$.

The MPC scheme incorporating Lyapunov exponents results in stable operation of the system. The temperature of the reactor is increased continuously whilst staying below the maximum allowable temperature at all times. As the approach of using a stability criterion leads to stable operation, the computational time is of major importance for industrial application.

The MPC scheme using a constant temperature set-point results, as expected, in stable operation of the systems. As will be shown below, keeping a constant temperature during the process results in a slow rate of conversion when compared to the other MPC schemes.

As can be seen in Figure 19 the processes controlled by MPC with an extended prediction horizon did not yield stable operation. This is observed due to the thermal runaway peaks reaching a maximum temperature of $T_R > T_{\text{chem}} = 470$ K, which therefore exceeds the maximum allowable temperature. This phenomenon occurs although a larger prediction horizon than for the MPC scheme incorporating Lyapunov exponents is used, because the standard nonlinear MPC scheme enters an unstable region without realising.

The first point of concern for this analysis is the computational cost required for each control scheme. This is of importance since these control schemes have to be implemented in an industrial setting. The lower the computational cost for each iteration, the more likely a successful implementation for online control schemes. In Table 7 the computational cost for each control scheme and process are given.

Table 7: Computational cost for each control scheme applied to processes $P_1^1 - P_6^1$. For the standard MPC scheme with an extended prediction horizon only the iterations before loss of stability are taken into account.

	Computational time / CPU s					
MPC scheme	P_1^1	P_2^1	P_3^1	P_4^1	P_5^1	P_6^1
With Lyapunov exponents	3.4	2.6	4.4	5.5	6.9	2.9
Constant set-point temperature	0.84	0.82	0.76	0.90	0.93	1.1
Standard MPC with extended horizon	7.9	6.2	6.2	7.6	7.3	8.8

The intensification of batch processes is one of the main aims of this work. To demonstrate this feature, the conversion profiles for all the above processes are shown. The target conversion with respect to component A is set to 80% such that the performance of each MPC scheme can be compared.

The conversion profiles for processes P_1^1 and P_2^1 are shown in Figure 20.

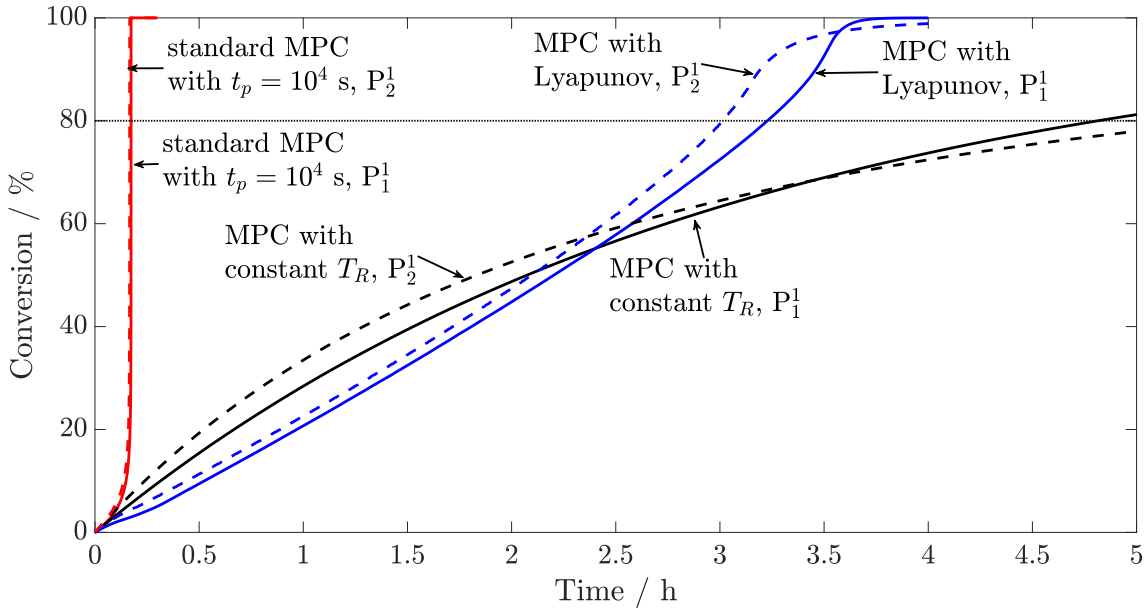

Figure 20: Conversion profiles of component A for each MPC scheme applied to processes P_1^1 and P_2^1. Solid lines correspond to process P_1^1, dashed lines to P_2^1. The dotted line represents the target conversion of 80%.

When using Lyapunov exponents the conversion increases continuously during each process. The MPC scheme using Lyapunov exponents results in reaching the target conversion after 3.2 h for process P_1^1 and after 3 h for process P_2^1.

The use of standard nonlinear MPC with an extended prediction horizon of $t_p = 10^4$ s yields a thermal runaway for P_1^1 and P_2^1: the conversion reaches 100% in a very sharp manner after 0.2 h for both process P_1^1 and process P_2^1.

Using a constant temperature set-point gives a very slow increase in conversion, not reaching the target conversion of 80% after approximately 5 h for processes P_1^1 and P_2^1.

The conversion profiles for processes P_3^1 and P_4^1 are shown in Figure 21.

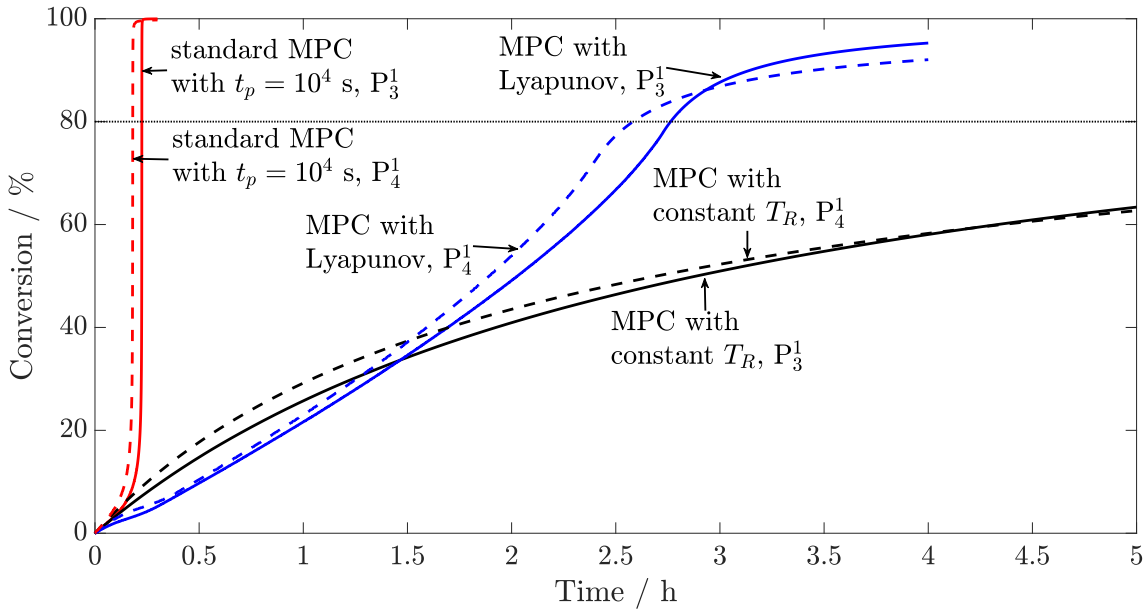

Figure 21: Conversion profiles of component A for each MPC scheme applied to processes P_3^1 and P_4^1. Solid lines correspond to process P_3^1, dashed lines to P_4^1. The dotted line represents the target conversion of 80%.

The control scheme using Lyapunov exponents gives a controlled increase in conversion, reaching the target conversion after 2.7 h for process P_3^1, and after 2.5 h for process P_4^1.

As can be seen in Figure 21 a constant temperature set-point does not achieve any intensification of the process. The target conversion of 80% is reached after 12 h for process P_3^1 and after 15 h for process P_4^1. The full timescale for these processes is outside the range shown in Figure 21 and omitted for clarity.

Thermal runaways are obtained when using the standard MPC scheme with a prediction horizon of $t_p = 10^4$ s. The maximum conversion of 100%, coinciding with the temperature peaks in Figure 21, occur at $t = 0.1$ h for process P_3^1 and at $t = 0.2$ h for process P_4^1.

The conversion profiles for processes P_5^1 and P_6^1 are shown in Figure 22.

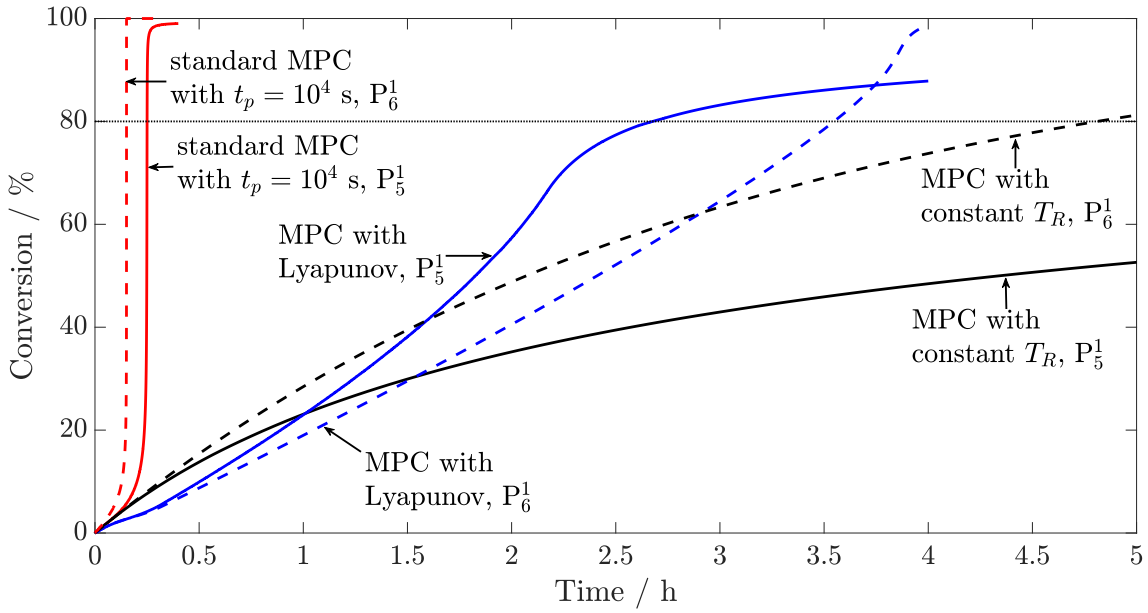

Figure 22: Conversion profiles of component A for each MPC scheme applied to processes P_5^1 and P_6^1. Solid lines correspond to process P_5^1, dashed lines to P_6^1. The dotted line represents the target conversion of 80%.

The MPC schemes implementing Lyapunov exponents for the system temperature give a steady increase in conversion. For this MPC scheme the target conversion of 80% is reached after 2.6 h for process P_5^1 and after 3.5 h for process P_6^1.

A constant set-point temperature again gives a very slower reaction rate, reaching the target conversion after 36 h for process P_5^1 and after 4.9 h for process P_6^1. The simulation horizon given in Figure 22 is not extended to this extent, as the graphs of major interest could not be observed otherwise.

Not using stability criteria, but an extended prediction horizon for standard MPC formulations again gives thermal runaway reactions: the conversion reaches a maximum value of 100% after 0.1 h for process P_5^1 and 0.2 h for process P_6^1.

From all the processes considered in this section, the processes using a constant temperature set-point required the lowest computational time, but the rate of conversion was very slow. The resulting processes were all stable, as no increase in reactor temperature occurred.

The standard nonlinear MPC scheme with an extended prediction horizon did not manage to keep the processes under control: thermal runaways occurred for all processes using this control strategy. Hence using such a control scheme to intensify batch processes is not feasible. With a prediction horizon of twice the size of that used for the MPC scheme with Lyapunov exponents, the computational time is already higher than that of the other MPC schemes. Hence, further increasing the prediction horizon to obtain stable operation will result in an even slower MPC scheme, making it less efficient for industrial application.

The MPC scheme using Lyapunov exponents results in stable operation of batch processes, while intensifying the reaction by continuously increasing the system temperature. The maximum temperature of $T_{\text{chem}} = 470$ K is never exceeded. The time required to reach the target conversion when compared to the constant temperature set-point processes is reduced by at least 1.5-fold. This demonstrates the value of using stability criteria within MPC frameworks.

From the computational time it is seen that the MPC scheme using Lyapunov exponents results in a lower computational time than the standard MPC scheme. The MPC scheme using Lyapunov exponents is faster, as the prediction horizon is much smaller. The information about stability is obtained by the Lyapunov exponents directly. Using a constant temperature set-point gives the smallest computational time, but no process intensification can be achieved with this MPC scheme.

Hence, using Lyapunov exponents gives an MPC scheme which can intensify such processes, whilst reducing the computational time when compared to standard MPC schemes. How these results change with more complex reaction schemes is discussed in the following section.

4.2.2. Intensification of reaction scheme 2

The three MPC schemes presented above are applied to processes $\mathrm{P}_1^2 - \mathrm{P}_6^2$ in the same way as for processes $\mathrm{P}_1^1 - \mathrm{P}_6^1$. Again, the maximum allowable temperature is set to $T_{\text{chem}} = 470\,\mathrm{K}$, and the target conversion is set to 80%. The resulting temperature profiles for processes P_1^2 and P_2^2 are shown in Figure 23.

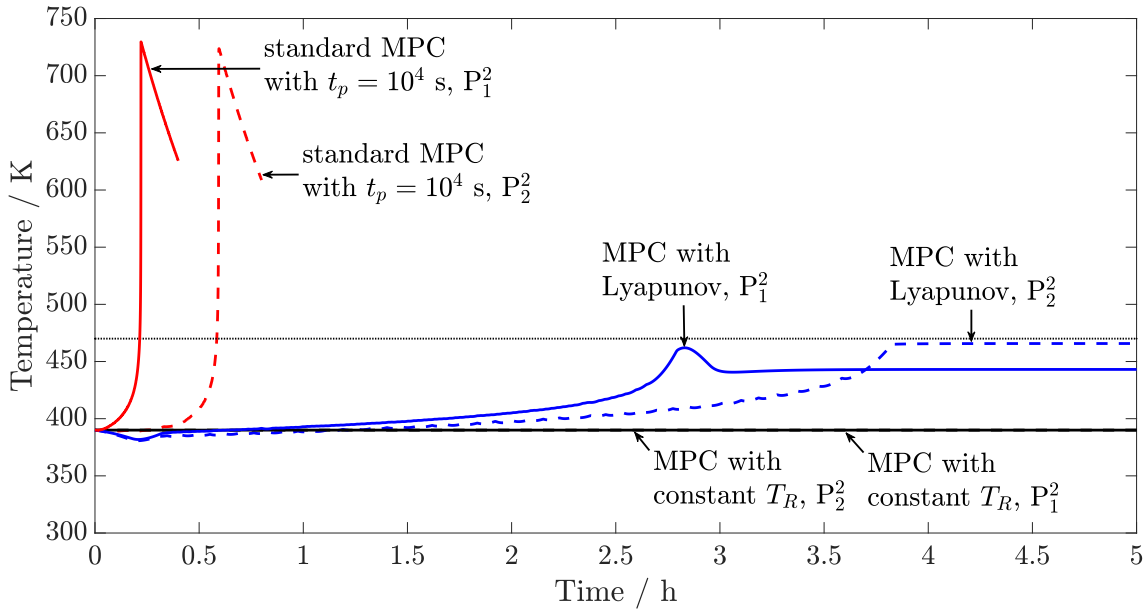

Figure 23: Temperature profiles for each MPC scheme applied to processes P_1^2 and P_2^2. Solid lines correspond to process P_1^2, dashed lines to P_2^2. The dotted line represents the maximum allowable temperature given by $T_{\text{chem}} = 470\,\text{K}$.

The MPC scheme incorporating Lyapunov exponents results in stable operation of the system. The reactor temperature increases in a steady manner until the maximum temperature is reached, without violating this constraint.

A constant temperature set-point for the standard MPC implementation gives steady operation for processes P_1^2 and P_2^2. No thermal runaway occurs for these processes, as the temperature is not increased during the operation.

The standard nonlinear MPC scheme using an extended prediction horizon does not yield stable operation. This is observed due to the thermal runaway peaks reaching a maximum temperature of T_R =730 K for processes P_1^2 and P_2^2, therefore exceeding the maximum allowable temperature. The temperature profiles for each MPC implementation applied to processes P_3^2 and P_4^2 are shown in Figure 24.

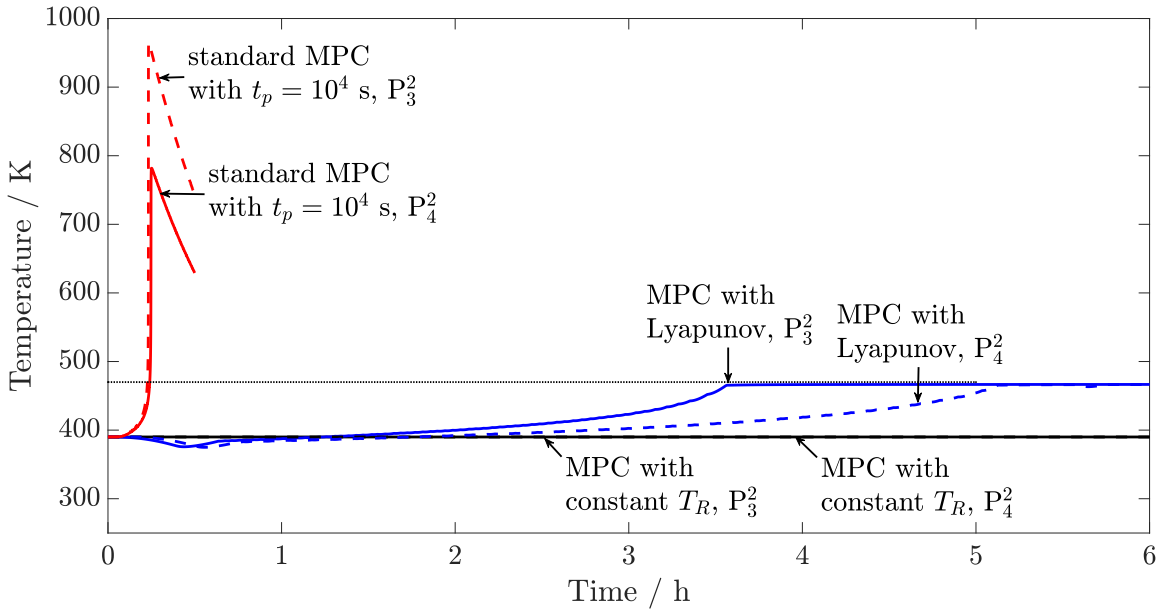

Figure 24: Temperature profiles for each MPC scheme applied to processes P_3^2 and P_4^2. Solid lines correspond to process P_1^2, dashed lines to P_2^2. The dotted line represents the maximum allowable temperature given by $T_{\text{chem}} = 470\,\text{K}$.

When embedding Lyapunov exponents within a standard MPC framework results in stable operation of processes P_3^1 and P_4^1. The reactor temperature is increasing continuously until the maximum allowable temperature is reached.

Using a constant temperature set-point results in stable operation, as can be seen in Figure 24. Due to the constant temperature it is expected that the rate of conversion for this control strategy is slower than for the other MPC structures.

The resulting temperature profiles when using standard MPC schemes without a stability criterion show thermal runaway behaviour. The peak temperatures for processes P_3^1 and P_4^1 are $T_R = 790\,\text{K}$ and $T_R = 950\,\text{K}$, respectively, exceeding the maximum allowable temperature. As for the MPC implementation for reaction scheme 1, this is not an acceptable control behaviour. The temperature profiles for each MPC implementation applied to processes P_5^2 and P_6^2 are shown in Figure 25.

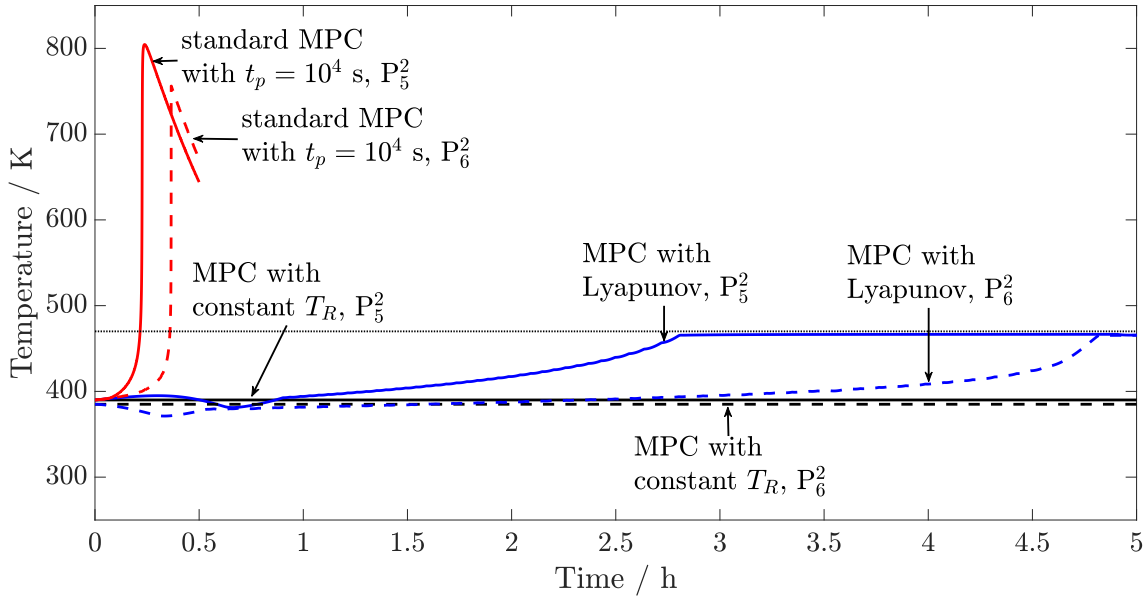

Figure 25: Temperature profiles for each MPC scheme applied to processes P_5^2 and P_6^2. Solid lines correspond to process P_1^2, dashed lines to P_2^2. The dotted line represents the maximum allowable temperature given by $T_{\text{chem}} = 470\,\text{K}$.

The MPC schemes incorporating Lyapunov exponents result in stable operation of the system. The temperature of the reactor is kept below the maximum, while increasing in order to give a faster rate of convergence.

A constant temperature set-point, as expected, gives stable operation of the batch reactor systems. The trade-off for this control scheme is the slow rate of conversion, which is demonstrated in the conversion profiles below.

In Figure 25 it can be seen that unstable operation is the result of a standard MPC framework with an extended prediction horizon for processes P_5^2 and P_6^2. The thermal runaway peaks reach a maximum temperature of $T_R = 800$ K and $T_R = 760$ K for processes P_5^2 and P_6^2, respectively, exceeding the maximum allowable temperature.

As the kinetic frameworks of the batch reactor system become more complex, it is expected that the computational cost also increases. Hence, the computational time of each MPC implementation for the more complex parallel reaction scheme is shown in Table 8.

Table 8: Computational cost for each control scheme applied to processes $P_1^2 - P_6^2$. For the standard MPC scheme with an extended prediction horizon only the iterations before loss of stability are taken into account.

	Computational time / CPU s					
MPC scheme	P_1^2	P_2^2	P_3^2	P_4^2	P_5^2	P_6^2
With Lyapunov exponents	5.5	5.2	7.3	8.0	7.4	5.7
Constant set-point temperature	0.91	0.85	0.95	0.98	1.0	1.2
Standard MPC with extended horizon	11	10	9.5	8.9	7.9	12

The intensification of batch processes is the other major contribution of this work. For this purpose, the conversion profiles of component A for each process, when controlled by the three presented MPC schemes, are demonstrated below.

The conversion profiles for each MPC implementation applied to processes P_1^2 and P_2^2 is presented in Figure 26.

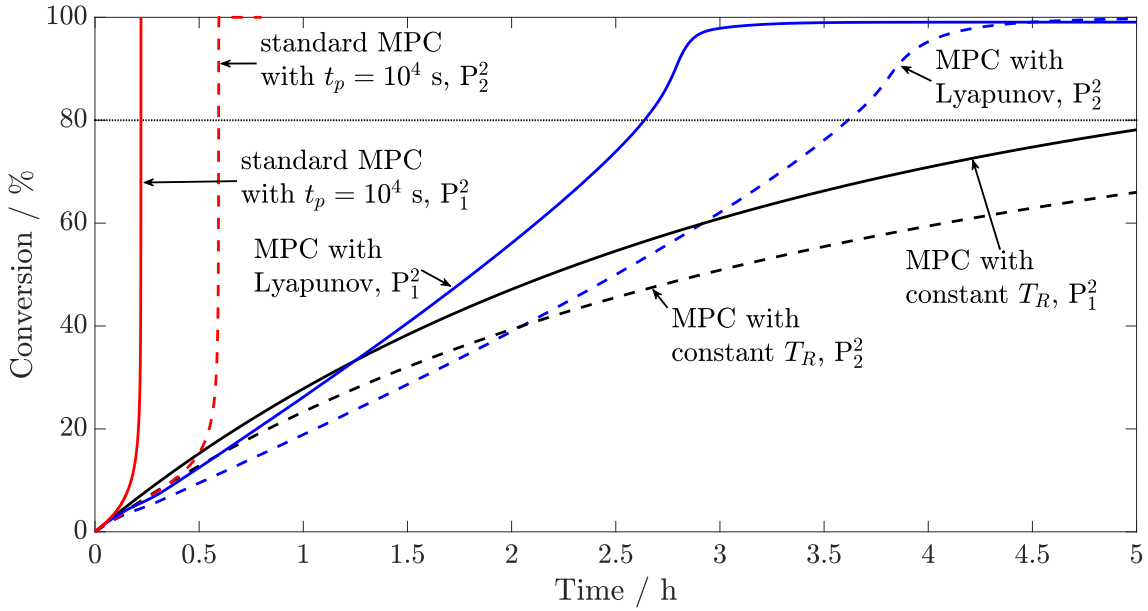

Figure 26: Conversion profiles of component A for each MPC scheme applied to processes P_1^2 and P_2^2. Solid lines correspond to process P_1^2, dashed lines to P_2^2. The dotted line represents the target conversion of 80%.

When using Lyapunov exponents the conversion increases continuously during each process, reaching the target conversion of 80% after 2.6 h for process P_1^2 and after 3.6 h for process P_2^2.

The use of an extended prediction horizon with $t_p = 10^4$ s for standard nonlinear MPC yields a thermal runaway, as can be seen in Figure 26. Full conversion of 100% is reached after only t =0.15 h for process P_1^2 and after t =0.55 h for process P_2^2.

Using a constant temperature set-point gives a very slow increase in conversion, reaching the target conversion of 80% after 5.1 h for process P_1^2 and 8.5 h for process P_2^2. For clarity this extended time frame is not shown here.

The conversion profiles for each MPC implementation applied to processes P_3^2 and P_4^2 are presented in Figure 27.

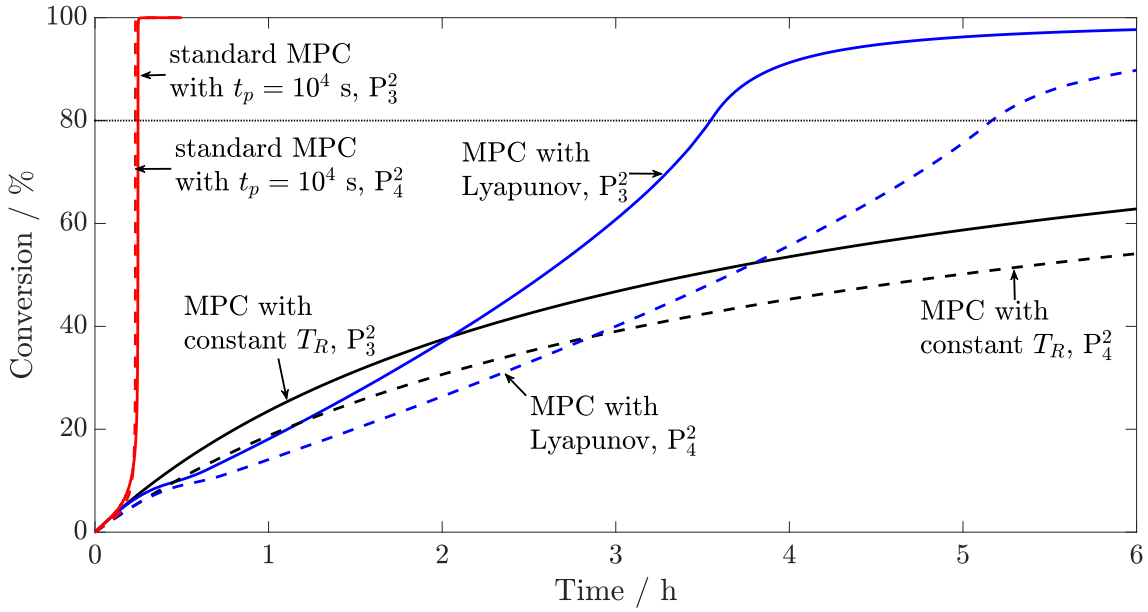

Figure 27: Conversion profiles of component A for each MPC scheme applied to processes P_3^2 and P_4^2. Solid lines correspond to process P_3^2, dashed lines to P_4^2. The dotted line represents the target conversion of 80%.

The MPC scheme embedding Lyapunov exponents gives a controlled increase in conversion, reaching the target after 3.5 h for process P_3^1, and after 5 h for process P_4^1.

In Figure 27 it can be seen that a constant temperature set-point does not achieve the target conversion within 6 h. The target conversion is reached after 15 h for process P_3^2 and 25 h for process P_4^2, but for clarity the time frame presented here is truncated to show the graphs of major interest.

Thermal runaways are obtained when using the standard MPC scheme with a prediction horizon of $t_p = 10^4$ s. The maximum conversion of 100%, coinciding with the temperature peaks in Figure 27, occurs at $t = 0.2$ h for process P_3^1, as well as for process P_4^1.

The conversion profiles for each MPC implementation applied to processes P_5^2 and P_6^2 is presented in Figure 28.

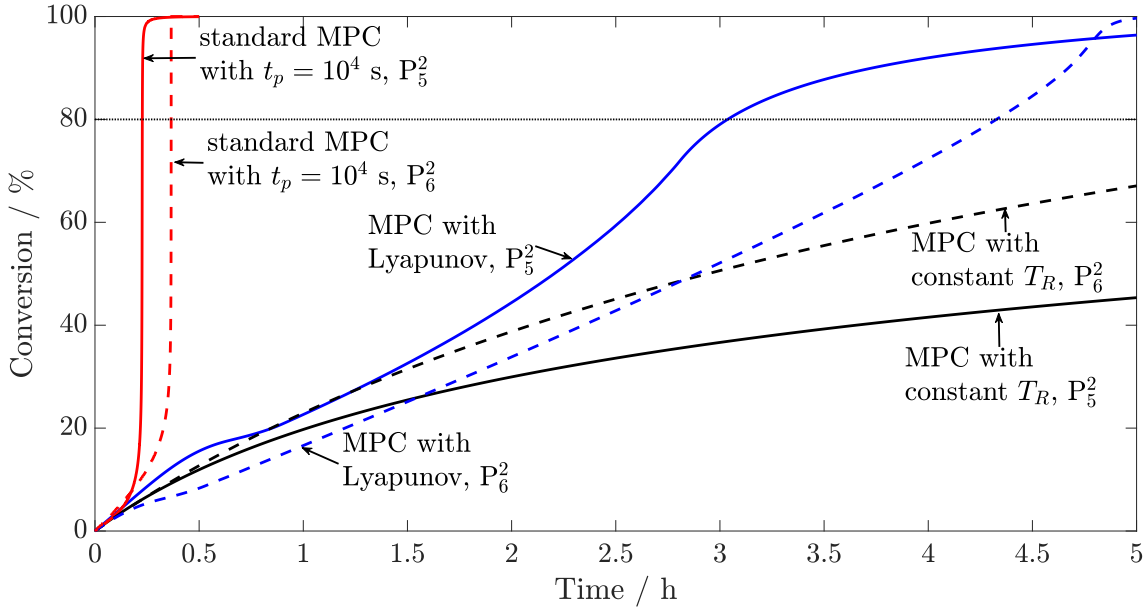

Figure 28: Conversion profiles of component A for each MPC scheme applied to processes P_5^2 and P_6^2. Solid lines correspond to process P_5^2, dashed lines to P_6^2. The dotted line represents the target conversion of 80%.

The MPC scheme embedding Lyapunov exponents gives a steady increase in conversion, reaching the target conversions of 80% after 3 h for process P_5^2, and after 4.2 h for process P_6^2.

A constant set-point temperature again gives a very slow reaction rate, not reaching the target conversion within the simulation horizon given in Figure 28. The target conversion is achieved after 7.5 h for process P_6^2, and is not reached within 50 h for process P_5^2. The complete profiles for these graphs are not shown in Figure 28 for clarity.

Thermal runaway behaviour is obtained if no stability criterion is embedded within the MPC framework and only the prediction horizon t_p is increased. This is observed on Figure 28, as 100% conversion is reached in a sharp manner after just 0.15 h for process P_5^2 and 0.35 h for process P_6^2.

As was observed for processes $P_1^1 - P_6^1$ a significant reduction in reaction time of at least 2-fold was achieved compared to constant set-point temperature processes when using Lyapunov exponents as a stability measure, embedded within an MPC framework. Furthermore, stable operation was always obtained which is not the case for standard MPC schemes with an extended prediction horizon.

The computational time of using Lyapunov exponents is shown to be smaller than for standard MPC schemes with large prediction horizon, but larger than for constant set-point temperature processes. As a larger prediction horizon would be required to give stable operation for the standard MPC approach, this would only increase the computational cost

further. Hence, using Lyapunov exponents can be used to intensify batch processes in a stable manner, while reducing computational cost. These results are in accord with the results obtained in Kähm and Vassiliadis (2018a).

4.2.3. Computational time and intensification of the nitration of toluene

One of the major advantages of using Lyapunov exponents for the system temperature to predict thermal stability is the ease of implementation: if a reliable process model with the generation of heat is present, which in all likelihood is the hardest part, the Lyapunov exponents can easily be evaluated even for very complex reaction networks. To showcase this the nitration reaction described in Sections 2.1.3 and 2.3.3 is considered next.

The aim of this case study is to prove that Lyapunov exponents embedded in MPC algorithms can be applied to more complex reaction networks, for which an intensification can be achieved while keeping the process under control. For this purpose, the nitration reaction presented above is simulated for different initial temperatures, while the maximum allowable temperature is set to $T_{\text{chem}} = 510$ K. The resulting temperature and conversion profiles are presented below, as well as the computational time of using each MPC scheme.

Due to the additional stability constraint, the objective of the optimal control problem in Equation (4.1a) can be changed to result in the most efficient process:

$$\min_{q_C(t)} \Phi^{(i)}\left(x\left(t\right), q_C\left(t\right)\right) = -\left[\text{o-}C_7H_7NO_2\right]\left(t_f^{(i)}\right) \tag{4.2}$$

where $\left[\text{o-}C_7H_7NO_2\right]\left(t_f^{(i)}\right)$ is the concentration at final time $t_f^{(i)}$ of the product, given by ortho-nitrotoluene, hereafter referred to as o-nitrotoluene. This optimisation tries to optimise the final concentration of o-nitrotoluene at each step of the MPC algorithm. Hence an optimisation of the product concentration is carried out with respect to constraints forcing the system to stay below the maximum allowable temperature, $T_{\text{chem}} = 510$ K, and keeping the system stable. This is not possible for standard MPC schemes, which if such an objective was given, would easily run into an unstable region resulting in a thermal runaway, as shown in Sections 4.2.1 and 4.2.2.

As there are four reagents and one temperature influencing the rate of heat generation in this system, a total of five Lyapunov exponents have to be evaluated at each step. The influence of increasing the number of relevant system variables on the computational time is analysed below. The resulting computational time will show how close this method is to the limit of applicability in an industrial setting.

The underlying MPC scheme uses a control horizon of $t_c = 30$ s with three equal control steps, and a prediction horizon of $t_p = 30$ s, hence not going beyond the control horizon. Since only the first MPC step is implemented, it is required that the computational time

does not exceed 10 s, which is the duration of the first control step. Otherwise this method is not fast enough to be implemented in industry.

The intensification is highlighted by comparing the concentration profiles of the products when using MPC with Lyapunov exponents to MPC processes with constant set-point temperatures. The MPC settings are the same here as they were for the second MPC scheme presented in Section 4.1.

The resulting temperature profiles for the addition reaction with MPC and Lyapunov exponents are given in Figure 29.

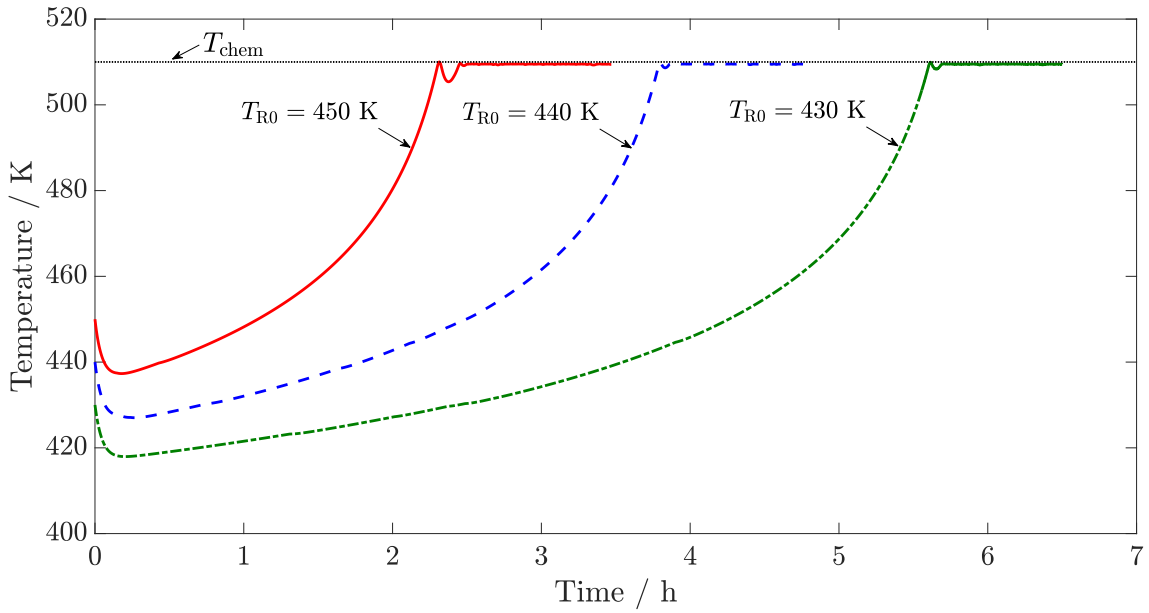

Figure 29: Temperature profiles of nitration reaction using an MPC scheme including Lyapunov exponents with different initial temperatures. The solid line relates to $T_{R0} = 450$ K, the dashed line relates to $T_{R0} = 440$ K and the dash-dotted line relates to $T_{R0} = 430$ K.

As can be seen, for none of the different initial temperatures the maximum allowable temperature of 510 K is exceeded. This means that the MPC scheme with Lyapunov exponents successfully controls each process even as the initial temperature increases, which makes the reaction inherently less stable. The temperature can hence be increased continuously in a flexible manner along the stable reaction path defined by the Lyapunov exponents with the optimal parameter settings found earlier.

The resulting temperature profiles when keeping a constant temperature set-point with MPC are shown in Figure 30.

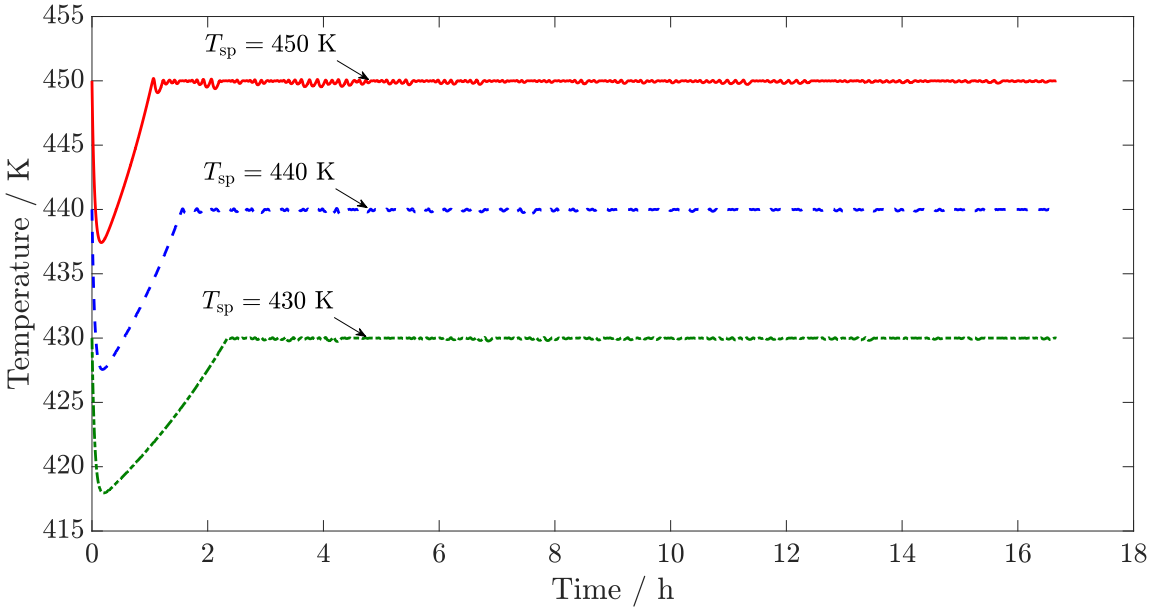

Figure 30: Temperature profiles of nitration reaction using an MPC scheme with constant set-point temperatures. The solid line relates to $T_{sp} = 450$ K, the dashed line relates to $T_{sp} = 440$ K and the dash-dotted line relates to $T_{sp} = 430$ K.

From Figure 30 it can be seen that constant temperature set-points lead to stable processes. This is the case as long as the start point of the process is not unstable, which would lead to thermal runaway behaviour.

As for this complex reaction scheme the computational time at each iteration is of great importance, the average CPU seconds required per iteration for each MPC scheme are shown in Table 9.

Table 9: Computational time for each MPC scheme applied to the nitration of toluene. For the unstable MPC scheme only the iterations before loss of stability are taken into account.

Initial temperature of MPC scheme	Computational time / CPU s
$T_{R0} = 430$ K	8.9
$T_{R0} = 440$ K	8.5
$T_{R0} = 450$ K	9.1

The respective concentration profiles for each MPC system with Lyapunov exponents are shown in Figure 31.

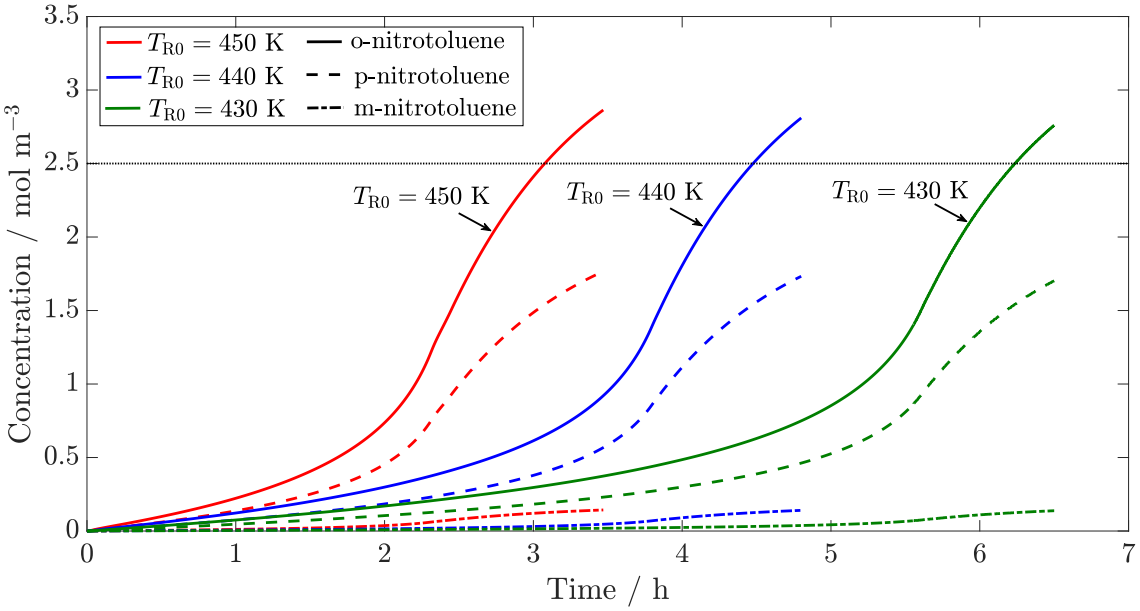

Figure 31: Concentration profiles of nitration reaction using an MPC scheme including Lyapunov exponents with different initial temperatures. The dotted line indicates the target concentration of o-nitrotoluene.

As the temperature for each process increases, the rate of increase in conversion increases. The target concentration for o-nitro-toluene of 2.5 mol m^3 is reached after at most 6 h for all analysed processes. Furthermore it can be seen that a higher initial temperature leads to faster convergence. In order to quantify the extent to which these reactions are intensified, the constant set-point temperature processes are considered next.

The concentration profiles for constant set-point temperatures within standard MPC schemes are shown below in Figure 32.

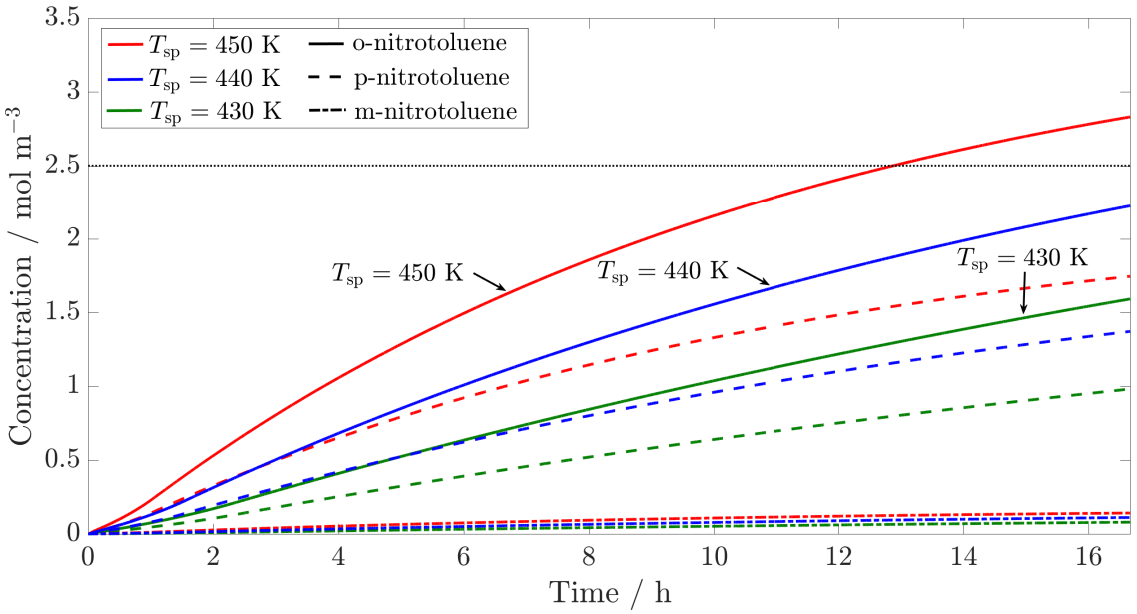

Figure 32: Concentration profiles of nitration reaction using an MPC scheme with constant set-point temperatures and with different initial temperatures. The dotted line indicates the target concentration of o-nitrotoluene.

Comparing Figures 32 and 31 highlights the intensification achieved by using an MPC scheme with Lyapunov exponents: the concentration for o-nitrotoluene only reaches the target concentration of 2.5 mol m^3 after 13 h for a set-point temperature of 450 K. A lower set-point temperature does not reach the target concentration within 16 h. Hence an intensification of at least two-fold is achieved. To show the dynamic behaviour of these processes, the time frame is truncated up to 16.5 h.

Figures 29 – 32 prove that using Lyapunov exponents as a stability measure for complex reaction kinetics works just as well as it does for simple reactions.

The computational time is just below the upper limit of 10 s, hence showing the feasibility of this method. These results show that the limit of applicability of this method, implemented as outlined above, is reached. Considerable improvements for computational time are necessary in order to implement this in an industrial setting, where continuous parameter estimation before the MPC stage could be necessary, requiring computational time as well. Hence, further improvements with respect to computational time are essential for a successful implementation in industry. Nevertheless, the batch processes of this industrially relevant reaction can be intensified by the application of Lyapunov exponents within standard MPC schemes.

For the reduction of computational time the underlying process model can potentially be simplified. This can be done by removing reactions and components not contributing greatly

to the overall system behaviour.

In this work the evolution of the stability is of major importance. The Lyapunov exponent with respect to the temperature gives the best indication of the system, which is based on the energy balance of the reactor. In the energy balance the contribution of each reaction i is weighted according to its fraction of the total heat generation, $r_i \, \Delta H_{r,i} / \sum_m (r_m \, \Delta H_{r,m})$. Consider the rate of heat generation of the nitration reaction starting at $T_{R0} = 440\,\mathrm{K}$, plotted in Figure 33 for the complete reaction mechanism, as well as the simplified one introduced below.

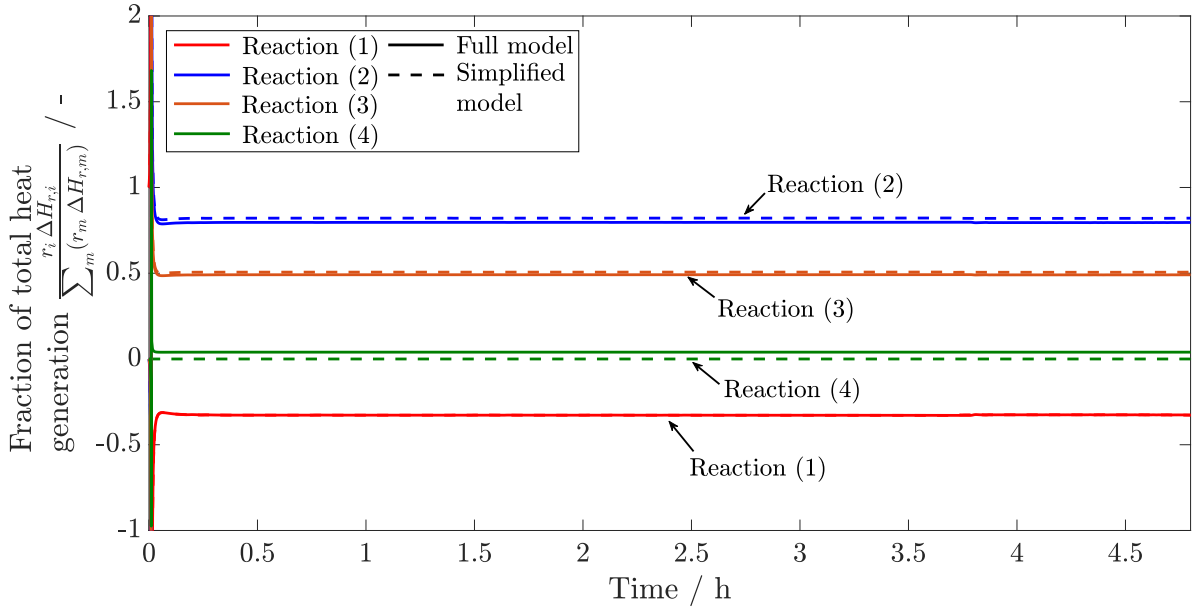

Figure 33: Fraction of total heat generation by each individual reaction for the complete and simplified reaction models. The solid lines represent the full mode, the dashed lines the simplified model.

The sum of each fraction of total heat generation adds up to one. In this reaction network an endothermic reaction is present, hence reaction (1) has a negative fraction of total heat generation throughout. Furthermore, in the first 150 s of the reaction, the individual fractions of total heat generation can be larger than +1 and smaller than -1, as the sum of all reactions still adds up to one.

The fraction of total heat generation for the formation of p-nitrotoluene, given by reaction (4), is below 3% for the full reaction model, as can be seen in Figure 33. Hence, to reduce the computational time, this particular reaction is removed in order to simplify the reaction model and reduce computational time.

The profiles of each fraction of total heat generation for the simplified reaction model are shown as dashed lines in Figure 33. From the dashed lines it can be seen, that the heat

generation of reaction (4) is zero, whilst the profiles of the other reactions follow the profiles of the full reaction model closely.

The temperature profiles of the complete reaction model, as well as the simplified model, are shown in Figure 34.

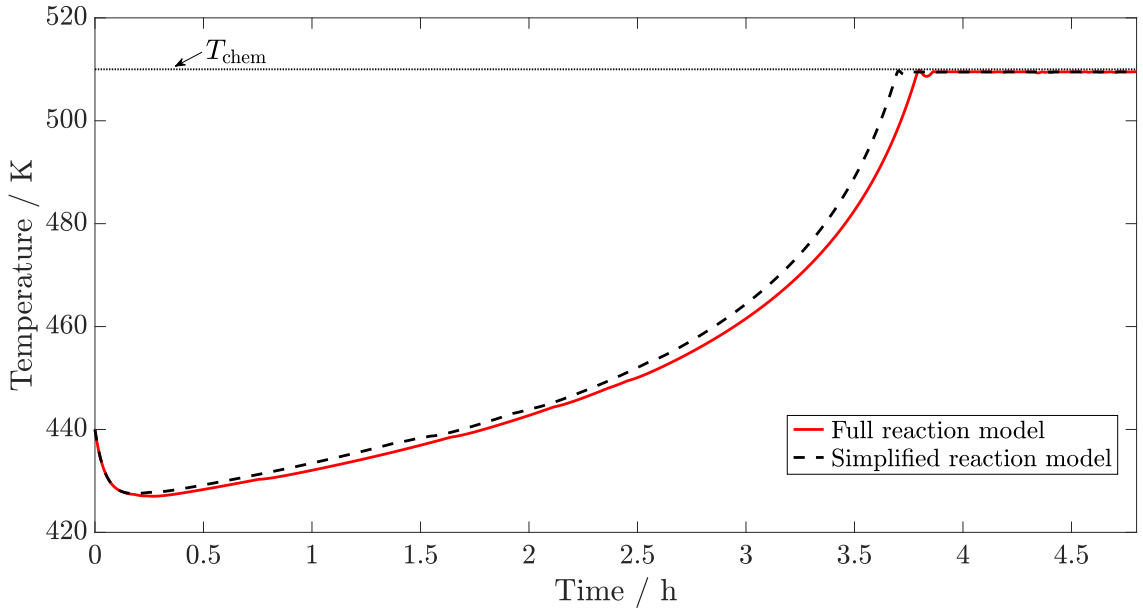

Figure 34: Temperature profiles for the complete and simplified reaction models. The solid line represent the full mode, the dashed line represents the simplified model.

As can be seen in Figure 34 the temperature profiles are very similar. In actual fact, the simplified model predicts a sharp temperature increase before the full model. Therefore, assuming the formation of p-nitrotoluene is negligible with respect to the overall reaction behaviour is valid.

The computational time required by each simulation is presented in Table 10.

Table 10: Computational time of the MPC scheme with Lyapunov exponents for the full and simplified nitration reaction models.

Reaction model	Computational time / CPU s
Full	8.5
Simplified	7.6

As can be seen in Table 10 the computational time saved by reducing the complexity of the reaction model is 0.9 s. Therefore, simplifying the reaction model does indeed reduce the computational time. Hence, considering which reactions give rise to instability due to their

contribution to the total heat generation becomes important with more complex reaction schemes.

5. Conclusions

An introduction to measuring system stability of batch processes with Lyapunov exponents is given. The batch reactor system simulated in this work is presented, with all the equations describing the dynamic behaviour of such systems. Two kinetic reaction schemes are given, for which a detailed analysis of the application of Lyapunov exponents is carried out. The nitration of toluene is considered as a relevant case study, showing interesting thermal runaway behaviour if not controlled well.

The theory underlying Lyapunov exponents is discussed in detail, outlining how the initial perturbation ϵ and time horizon t_{lyap} defining local Lyapunov exponents are chosen optimally with the help of sensitivity analyses. PI control is applied to the batch reactor system introduced: an initially stable process is made unstable by increasing the set-point temperature in a step-wise manner. Hence a transition from stable to unstable operation is obtained. It is found that the Lyapunov exponents affecting the heat generation of the reaction are most relevant to the system stability. Therefore the number of Lyapunov exponents used can be decreased.

Model Predictive Control (MPC) is introduced as an advanced control scheme and alternative to traditional PI(D) control. The ability to include system constraints enables the inclusion of stability measures for improved system control and process intensification. It is found that including Lyapunov exponents as additional system constraints yields intensified batch processes kept under control at all times. A continuous increase in system temperature by increasing the prediction horizon of a standard MPC scheme gives unstable control, leading to thermal runaway behaviour. Constant set-point temperature processes, commonly found in industry, are under control but the rate at which the target conversion is reached is very slow in comparison.

Furthermore, a reduction in computational time is achieved when using this stability criterion as opposed to an increased prediction horizon. The resulting MPC scheme implementation is fast enough for reactions with up to 5 relevant variables, although MATLAB$^{\mathrm{TM}}$ is being used. Hence it should be noted that as the number of system variables analysed using Lyapunov exponents increases, the computational time required per MPC step increases significantly. Using other programming languages, e.g. C++ or FORTRAN, can give a significant reduction in computational cost. The use of parallel computing for the constraint evaluation will also be investigated to improve computational efficiency.

The computational time can be was shown to be reduced by simplifying the reaction

kinetics underlying the system according to the contribution of each reaction to the total heat generation, which becomes important as the model becomes more complex.

Setting Lyapunov exponent values as hard constraints within the OCP formulation in Equation (4.1a) can potentially lead to infeasibility. In such a scenario the cooling capacity is increased as much as possible according to Equation (4.1d), as this is the most stabilising action possible for the batch systems analysed. Increasing the control horizon to have more control increments with smaller time frames, such that maximum cooling capacity can be achieved at the end of the control horizon, would mitigate this issue and will be analysed in future work. Furthermore, additional theoretical considerations on the feasibility of the MPC formulations will be carried out in future work.

Incorporating a stability constraint as a hard constraint for continuous systems controlled by MPC has been considered in literature (Zhang et al., 2018; Albalawi et al., 2018, 2017). For such continuous systems with a particular operating point such a control scheme is not always necessary, as the stability of operating points even for strongly nonlinear systems can be proven theoretically with Lyapunov stability functions (Haßkerl et al., 2018; Griffith et al., 2017). The methods presented in Albalawi et al. (2016) are rigorous for continuous reactor systems. Applying such methods to batch reactors would be beneficial and are hence subject to future work.

Future work will focus on implementing Lyapunov exponents to other complex reaction kinetics of batch reactors. More advanced MPC schemes will be implemented to speed up the time required for each iteration. The effect of uncertainty in process parameters and model-plant-mismatch on the reliability of Lyapunov exponents have to be considered for future applications. The robustness of stability criteria for online applications is of major importance and hence needs consideration in future work.

Acknowledgments

We thank the Engineering and Physical Sciences Research Council (EPSRC) and the Department of Chemical Engineering and Biotechnology, University of Cambridge, for funding the EPSRC PhD studentship for this project.

References

Akpan, V. A., Hassapis, G. D., 2011. Nonlinear model identification and adaptive model predictive control using neural networks. ISA Transactions 50, 177–194.

Albalawi, F., Alanqar, A., Durand, H., Christofides, P. D., 2016. A feedback control framework for safe and economically-optimal operation of nonlinear processes. American Institue of Chemical Engineers Journal 62, 2391–2409.

Albalawi, F., Durand, H., Christofides, P. D., 2017. Process operational safety using model predictive control based on a process safeness index. Computers & Chemical Engineering 104, 76–88.

Albalawi, F., Durand, H., Christofides, P. D., 2018. Process operational safety via model predictive control: Recent results and future research directions. Computers & Chemical Engineering 114, 171–190.

Anagnost, J. J., Desoer, C. A., 1991. An elementary proof of the Routh-Hurwltz stability criterion. Circuits Systems Signal Process 10.

Anucha, S., Chayavivatkul, V., Banjerdpongchai, D., 2015. Comparison of PID control and linear model predictive control application to regenerative thermal oxidizer system. In: Control Conference (ASCC).

Barkelew, C., 1959. Stability of chemical reactors. Chemical Engineering Progress Symposium Series 25, 37–46.

Bohne, D., Fischer, S., Obermeier, E., May 2010. Thermal conductivity, density, viscosity, and Prandtl-numbers of ethylene glycol-water mixtures. Berichte der Bundesgesellschaft für physikalische Chemie 88 (8), 739–742.

Charitopoulos, V. M., Dua, V., 2016. Explicit model predictive control of hybrid systems and multiparametrix mixed integer polynomial programming 62, 3441–2460.

Chen, L.-P., Chen, W.-H., Liu, Y., Peng, J.-H., Liu, R.-H., 2008. Toluene mono-nitration in a semi-batch reactor. Central European Journal of Energetic Materials 5, 37–47.

Christofides, P. D., Liu, J., Muñoz de la Peña, D., 2011. Networked and Distributed Predictive Control. Springer, London, Ch. 2, pp. 13–45.

Chuong La, H., Potschka, A., Bock, H. G., 2017. Partial stability for nonlinear model predictive control. Automatica 78, 14–19.

Crittenden, J. C., Trussell, R. R., Hand, D. W., Howe, K. J., Tchobanoglous, G., 2012. MWH's Water Treatment: Principles and Design, 3rd Edition. John Wiley & Sons, Ch. Appendix C, pp. 1861–1862.

Davis, M., Davis, R., 2003. Fundamentals of Chemical Reaction Engineering. McGraw-Hill, Ch. 2, pp. 53–56.

DeHaan, D., Guay, M., 2010. Model Predictive Control. Sciyo, Ch. 2, pp. 26–58.

Dever, J., George, K., Hoffman, W., Soo, H., 2004. Kirk-Othmer Encyclopedia of Chemical Technology. John Wiley & Sons, Ch. Ethylene Oxide, pp. 632–673.

Green, D. W., Perry, R. H., 2008. Perry's Chemical Engineers' Handbook, eighth Edition. The McGraw-Hill, Ch. 2.

Griffith, D. W., Zavala, V. M., Biegler, L. T., 2017. Robustly stable economic nmpc for non-dissipative stage costs. Journal of Process Control 57, 116 – 126.

Haber, R., Bars, R., Schmitz, U., 2011. Predictive Control in Process Engineering. Wiley-VCH Verlag GmbH & Co. KGaA, Ch. 2, pp. 29–54.

Halder, R., Lawal, A., Damavarapu, R., 2008. Nitration of toluene in a microreactor. Catalysis Today 125, 74–80.

Haßkerl, D., Lindscheid, C., Subramanian, S., Diewald, P., Tatulea-Codrean, A., Engell, S., 2018. Economics optimizing control of a multi-product reactive distillation process under model uncertainty. Computers & Chemical Engineering, 1–24.

Hirschfelder, J. O., Curtiss, C. F., Bird, R. B., 1955. Molecular theory of gases and liquids. American Insitute of Chemical Engieers Journal 1 (2), 272.

Huang, R., Biegler, L. T., Harianth, E., 2012. Robust stability of economically oriented infinite horizon nmpc that include cyclic processes. Journal of Process Control 22, 51–59.

Hurwitz, A., 1895. Über die Bedingungen, unter welchen eine Gleichung nur Wurzeln mit negativen reellen Theilen besitzt. Math. Ann. 46 (2), 273–284.

Kähm, W., Vassiliadis, V. S., 2018a. Lyapunov exponents with model predictive control for exothermic batch reactors. In: IFAC-PapersOnLine. Vol. 51.

Kähm, W., Vassiliadis, V. S., 2018b. Thermal stability criterion integrated in model predictive control for batch reactors. Chemical Engineering Science 188, 192–207.

Lee, J. H., 1994. State-space interpretation of model predictive control. Automatica 30 (4), 707–717.

Lee, J. H., 2011. Model predictive control: Review of the three decades of development. Journal of Control, Automation, and Systems 9, 415–424.

Luo, K.-M., Chang, J.-G., 1998. The stability of toluene mononitration in reaction calorimeter reactor. Journal of Loss Prevention in the Process Industries 11, 81–87.

Mawardi, M., 1982. The nitration of monoalkyl benzene and the separation of its isomers by gas chromatography. Pertanika 5, 7–11.

Mayne, D. Q., 2014. Model predictive control: Recent developments and future promise. Automatica 50, 2967–2986.

Melcher, A., 2003. Numerische berechnung der lyapunov-exponenten bei gewöhnlichen differentialgleichungen. Ph.D. thesis, Universität Karlsruhe, Fakultät für Mathematik.

Nocedal, J., Wright, S., 2006. Numerical Optimization. Springer, Ch. 18, pp. 526–572.

Rawlings, J., Mayne, D., 2015. Model Predictive Control: Theory and Design. Nob Hill Publishing, Ch. 1, pp. 1–60.

Rossi, F., Copelli, S., Colombo, A., Pirola, C., Manenti, F., 2015. Online model-based optimization and control for the combined optimal operation and runaway prediction and prevention in (fed-)batch systems. Chemical Engineering Science 138, 760–771.

Routh, E., 1877. A treatise on the stability of a given state of motion: Particularly steady motion. Macmillan.

Semenov, N., 1940. Thermal theory of combustion and explosion. In: Progress of Physical Science (U.S.S.R). Vol. 23.

Shampine, L., Reichelt, M., Kierzenka, J., 1999. Solving index-1 daes in matlab and simulink. SIAM Review 41, 538–552.

Sheats, G., Strachan, A., 1978. Rates and activation energies of nitronium ion formation and reaction in the nitration of toluene in 78% sulphuric acid. Canadian Journal of Chemistry 56, 1280–1283.

Sinnot, R., 2005. Chemical Engineering Design. Vol. 6. Elsevier Butterworth-Heinemann, Ch. 12, pp. 634–638.

Strozzi, F., Zaldívar, J., 1994. A general method for assessing the thermal stability of batch chemical reactors by sensitivity calculation based on lyapunov exponents. Chemical Engineering Science 49 (16), 2681–2688.

Strozzi, F., Zaldívar, J., 1999. On-line runaway detection in batch reactors using chaos theory techniques. American Institute of Chemical Engineers Journal 45 (11), 2429–2443.

Teja, A. S., 1983. Simple method for the calculation of heat capacities of liquid mixtures. Journal of Chemical Engineering Data 28, 83–85.

Theis, A., 2014. Case study: T2 Laboratories explosion. Journal of Loss Prevention in the Process Industries 30, 296–300.

Zhang, Z., Wu, Z., Durand, H., Albalawi, F., Christofides, P. D., 2018. On integration of feedback control and safety systems: Analyzing two chemical process applications. Chemical Engineering Research & Design 132, 616–626.